CALCIUM SIGNAL PROPAGATION IN ASTROCYTES

SEAN BURROWS

MBXSB7

A thesis presented to the School of Life Science

University of Nottingham

MRes Neuroscience

February 2021

Dr Tomas Bellamy

Dr Paul Smith

Abstract

Astrocytes are glial cells that play many roles in maintaining homeostasis of the central nervous system and modulating both vascular and neuronal networks. Astrocytes express a range of neurotransmitter receptors that allow for communication from the neuron to astrocyte and mediate feedback and modulation of signal transmission at the synapse. Astrocyte calcium signalling caused by receptor activation is responsible for the release of gliotransmitters capable of modulating synaptic activity. The calcium signals of the glia have complex spatiotemporal properties that range from transients, isolated to astrocyte microdomains, to wide intracellular calcium waves capable of propagating within cellular networks. The range that the calcium response covers will determine how many synapses (and blood vessels) could be modulated by feedback from glia. In this study we investigated the factors that control signal propagation in astrocytes using two experimental models: cultured primary astrocytes, and Bergmann glial cells in acutely isolated cerebellar slices.

Initially, primary cultures of astrocytes loaded with Fluo-5F indicator were used to investigate whether ATP release from astrocytes contributed to the calcium response generated by the excitatory neurotransmitter, glutamate. A broad-spectrum antagonist of P2 receptors (PPADS) did not affect either the initial response of astrocytes to glutamate exposure, or the ongoing oscillations in calcium observed during a late stage of continuous stimulation. We next screened purinergic receptor antagonists to identify the receptors linked to ATP responses in the cells, and showed that responses in cultured cells were most sensitive to suramin.

Next, we developed a method to bulk load acutely isolated cerebellar slices with Fluo5F in order to examine Bergmann glial responses to stimulation, without the need for patch clamp recordings. The unipolar morphology of cerebellar Bergmann glia, with long fibres that project microdomains to enclose the synapses throughout the molecular layer of the cerebellar cortex, allows the spatial range of calcium signals to be visualised. Here responses to parallel fibre stimulation were investigated by using spatial and temporal components to isolate the Bergmann glia contribution to the overall fluorescence changes.

Short bursts of electrical stimulation of the parallel fibres at 30-100 Hz in 5-10 pulses reliably generates calcium responses within the Bergmann glia that spread along the Bergmann fibres, and are sensitive to pharmacological inhibition by PPADS (P2 receptor antagonist), CPCCOEt (mGluR1 receptor antagonist) and NBQX (AMPA receptor antagonist). We were able to reproduce these results from single cell recordings using the bulk loading technique, suggesting that the glial signal can be effectively detected from the mixed population of cells in the molecular layer. In contrast to cultured cells, however, suramin had little impact on calcium signals in Bergmann glia, indicating that results from primary culture cannot be generally translated into other, more intact, preparations.

Previous work within our laboratory has shown that stimulation of the parallel fibres with a protocol that induces long term potentiation at the synapse (16 Hz for 15 s) dramatically decreases the spatial range of the Bergmann glia calcium responses generated by the 30 Hz tetanus. This result suggests “spatial plasticity” may be a feature of glial calcium signalling. This depression of 30 Hz responses was also reproduced with the bulk loading method, and we finally used a broad-spectrum serotonergic receptor antagonist, asenapine, to test the

hypothesis that serotonergic signalling contributes to the glial spatial plasticity. However, there was no statistically significant effect.

We have successfully validated a less technically demanding method for monitoring the Bergmann glia calcium responses within slices and confirmed the principle for screening signalling pathway candidates that could affect the spatial range and plasticity of astroglial calcium signals. This should accelerate progress in understanding how the pattern of synaptic activity in a neuronal network is related to the range of calcium signals generated in adjacent glial networks.

1 Introduction

Glial cells constitute half of all cells in the central nervous system and are electrically passive, differentiating them from neurons. Although glial cells were identified in the nineteenth century, their roles in the brain have become much better understood in the last few decades with the advent of fluorescence imaging techniques and transgenic methods (Araque, et al. 1999; Perea & Araque, 2005; Jäkel & Dimou, 2017; Stobart, et al. 2018). This has brought to light the importance of glial cells in the regulation of neuronal transmission and signal encoding, changing how we think about brain function and development.

Glial cells are a collection of cells that have distinct physiological features and phenotypes that can be differentiated into three main classes: oligodendrocytes, microglia and astrocytes. Oligodendrocytes are myelinating cells that form the sheath around neuronal axons improving conductance efficiency and speed (Jäkel & Dimou, 2017; Foerster, et al. 2019). Microglia are the resident immune cells of the brain (Alekseeva, et al. 2019). Astrocytes are the most abundant class of glia in the brain, and play multiple roles in maintaining homeostasis, immune response (through reactive gliosis) and regulation of both synaptic transmission and blood flow (Nedergaard, et al. 2003, Rose & Kirchhoff, 2015; Allen & Lyons, 2018).

1.1 Astrocytes

Astrocytes are versatile and abundant across the brain regions and were originally thought to play only roles in the structural integrity and homeostatic maintenance of the neuronal microenvironment. It is now understood that they can contribute to neurophysiology in many more active ways, even from the early stages of development when astrocytes contribute to the promotion of neurogenesis and synaptogenesis (Nedergaard, et al. 2003; Araujo, et al. 2019; Allen & Lyons, 2018).

Astrocytes adapt to the microenvironment of each brain region, displaying phenotypic heterogeneity. The development of astrocytes has shown a regional distinction for gene expression profiles and morphologies that is encoded by positional cues (Bayraktar, et al. 2014; Rose & Kirchhoff, 2015). Astrocytes appear to be specialized for each region to fulfil the requirements of the developing brain and future activity.

This can be observed in the astrocyte alignment and spatial densities varying across brain regions – with radial orientations in the cerebellum and retina compared to multidirectional “bush-like” appearance in the cortex and hippocampus (Rose & Kirchhoff, 2015; Pestana, et al. 2020). Mature astrocytes can form a dense mesh throughout the brain parenchyma, capable of widespread communication and modulation of the synaptic network that it encloses (Franke, et al. 1999; Fumagali, et al. 2003; Jacob, et al. 2014). These highly connected astroglial networks span volumes of neural tissue encompassing thousands of neurons (Perea, et al. 2009; Jacob, et al. 2014).

A physiological heterogeneity also shows differences in cell to cell signalling. For example, astroglia form a network of multiple cells connected via gap junctions formed by connexin proteins (Chever, et al. 2014), which allows the astrocytes to regulate the homeostasis of the extracellular space and also allows them to detect and respond to activity in the neuronal network over large distances (Fumagalli, et al, 2003). There have been shown to be differences

in coupling effectiveness between hippocampal and striatal astrocytes via connexin proteins (Pestana, et al. 2020), suggesting region variation in syncytium structure and function.

Intricate differences in calcium signalling exist among astrocyte populations that have been extensively investigated (Nedergaard, et al. 2003; Verkhratsky & Nedergaard, 2018; Pestana, et al. 2020). These have highlighted the neurotransmitter differentiation and signal association for astrocytes supporting neuronal development in immature brain regions (Nedergaard, et al. 2003; Pestana, et al. 2020). Furthermore, a recent look into transcriptomic diversity linked to the calcium signalling of astrocyte revealed clustering of cell types in layers or compartments of the cortex and hippocampus, to mediate specific physiological functions (Batiuk, et al. 2020).

Astroglia also form end feet on the blood vessels in the brain. This anatomical association allows them to regulate blood flow in response to increased activity in the synaptic network, allowing coordination of neuro-vascular coupling for energy supply and demand (Nedergaard, et al. 2003; Allen & Lyons, 2018).

1.2 Maintenance of Extracellular Microenvironment

Astrocytes have an important role in homeostatic regulation of the brain. Transmembrane ion channels and transporters in astrocytes aid in the maintenance of action potential propagation by buffering extracellular ion concentrations. Specifically, glia are capable of spatial buffering of K^+ ions through inward rectifying potassium channels (K_{ir}) and ion transporters or cotransporters (Wang, et al. 2012). This redistribution of ions prevents accumulation of extracellular K^+ released during action potential generation that could cause depolarisation of neighbouring neurons (Fleischer, et al. 2015). The uptake can modulate signal transduction of the neurons to prolong or inhibit neuronal output through K^+ redistribution (Butt & Kalsi, 2006; Wang, et al. 2012)

A second role for astrocytes is metabolic partitioning. Astrocytes contain glycogen granules and can supply energy to neurons by conversion of glycogen into lactate which can be used aerobically by neurons (Brown & Ransom, 2007). This “lactate shuttle” can provide energy during periods of high energy demands or hypoglycaemia but may also play a role under normal physiological conditions (Bélanger et al. 2011). Similarly, astrocytes regulate the redox environment in the brain, principally through maintenance of levels of antioxidant glutathione (Baxter & Hardingham 2016). Finally, astrocytes also release important precursors for neurotransmitter synthesis, such as glutamine (used for synthesis of glutamate and GABA) that neurons cannot produce themselves (Rose et al. 2013).

Astroglia also regulate the uptake and recycling of neurotransmitters from the extracellular space. For example, glutamate uptake mechanisms such as EAAT1 and EAAT2 (excitatory amino acid transporters) are expressed in astrocytes and are essential for terminating excitatory transmission (Figure 1.1) (Rose, et al. 2018). In the instance of glutamate, dysregulation of uptake can cause excitotoxicity, which can contribute to neuronal death involved in neurological diseases such as epilepsy (Ding, et al. 2007; Rose, et al. 2018).

Reuptake and recycling of transmitters extends beyond just glutamate with astrocytes capable of processing gamma-aminobutyric acid (GABA) (Jacob et al. 2014), serotonin (5-HT)

(Anderson, et al. 1992, Hirst, et al. 1998), adenosine (Peng, et al. 2005, Boison, et al. 2009) and numerous monoamines (Takeda, et al. 2002). The phenotypic plasticity of astroglia makes them capable of adapting to synaptic signalling of the neurons they ensheathe and the corresponding neurotransmitters. This occurs through selective transporter expression (Murphy-Royal, et al. 2015; Rose, et al. 2018) and the ability to migrate towards a synaptic release site (Grosche, et al. 2002; Lippmann Bell, et al. 2010), thereby ensuring the proximity of astrocyte receptors and transporters to the site of release. This not only has a neuroprotective effect by increasing the uptake and recycling of neurotransmitters but extends into the modulation of signalling at the synapse.

The uptake of the neurotransmitters plays a role in modulation of synaptic activity (De Zeeuw, and Hoogland. 2015). The glutamate transporters can directly affect specific local concentrations at the synapse, altering the time course of the synaptic transient. The expression of uptake mechanisms at the cell membrane can affect the duration and amplitude of glutamate transients at the postsynaptic neuron directly affecting signal propagation. This comes from a close link between neuronal-astrocyte signalling, in which activation of astrocyte surface receptors can regulate transporter mobility and expression (Murphy-Royal, et al. 2015; Rose, et al. 2018). The expression of neurotransmitter receptors by astrocytes therefore forms a mechanism for regulation of neurotransmitter clearance but also can lead to signalling within the astrocytes (Figure 1.1).

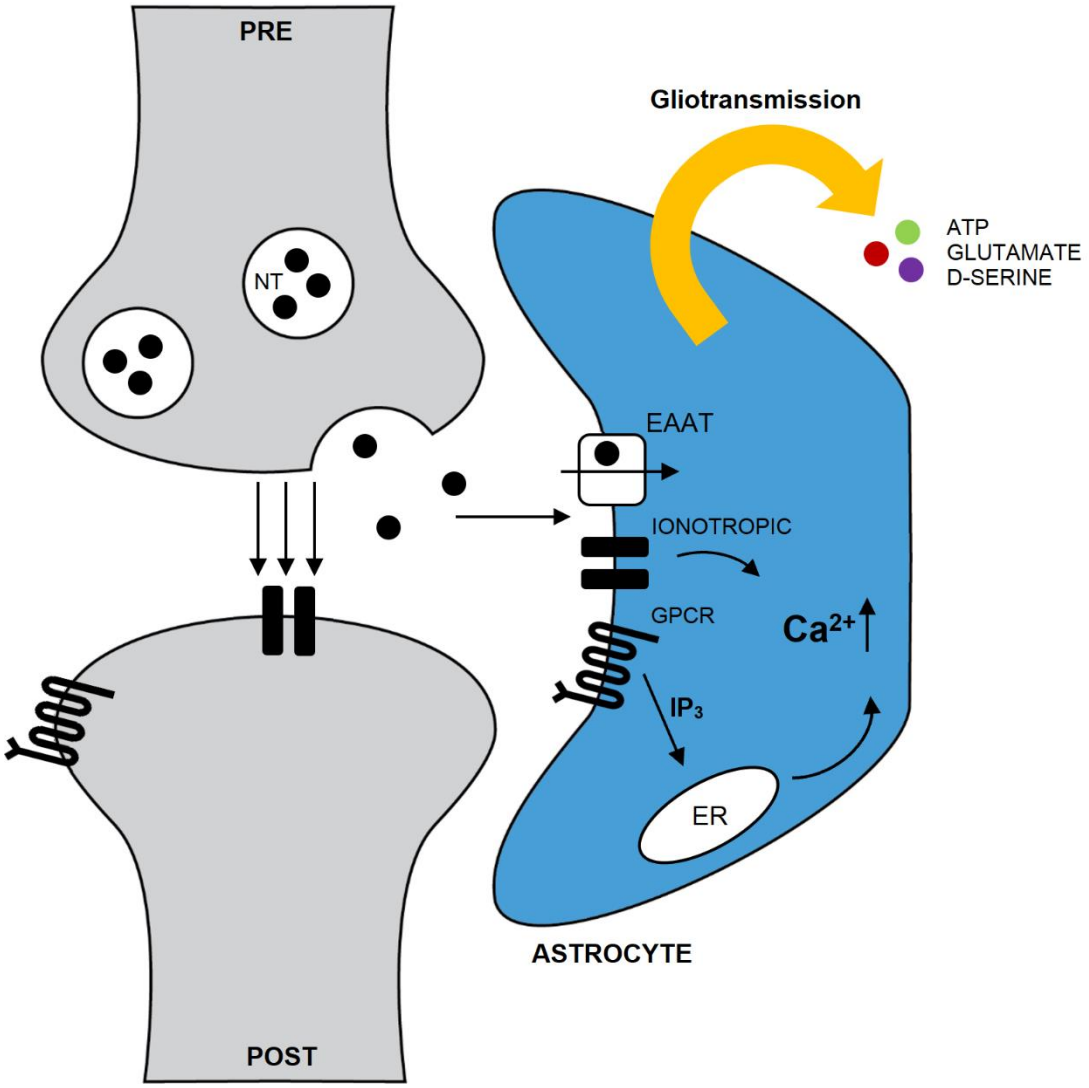

Figure 1.1. The tripartite synapse. Astrocytes become a third part of the synapse, providing important support and modulation for neuronal transmission. The formation of compartments around the synapse allow for focussing of signalling and prevent widespread diffusion of vesicular-released neurotransmitters (NT) from the synaptic cleft. Here astroglia can regulate neurotransmission through the uptake of extracellular transmitters released into the synaptic space. Transmitters (filled circles) are rapidly taken up and recycled by astrocyte. Mechanisms such as EAAT (EAAT1 & EAAT2) are expressed for the uptake of glutamate to end transmission and protect against excitotoxicity (Rose, et al. 2018). Astroglia can also detect and respond to the neuronally released transmitter. Transmembrane ionotropic and metabotropic receptors lead to a downstream calcium response in the astrocyte. Ionotropic receptors form a pore-like channel for rapid entry of Ca^{2+} ions. Metabotropic (GPCR) receptors, coupled to G_q proteins, increase IP_3 levels to act on endoplasmic reticulum (ER) membrane receptors triggering the release of Ca^{2+} from internal stores for larger increases in intracellular calcium. This calcium response can lead to the increased expression of these transmembrane proteins, either receptors or uptake mechanisms, to feedback to neurotransmission. The calcium response can propagate through the astroglia leading to a widespread response. One form of propagation is via gliotransmitter release (Orange Arrow). Here signalling molecules released from the astrocyte can activate neighbouring astrocytes for transglial calcium responses, potentially coordinating glial modulation of multiple synapses. This mechanism also allows for the astrocyte to regulate neuronal signalling as a form of bi-directional communication (Araque, et al. 1999, Perea & Araque, 2005). The primary gliotransmitters are ATP, Glutamate and D-serine, capable of acting on a wide range of targets (Araque, et al. 2014).

1.3 Astrocyte Signalling

Astrocytes express a wide range of neurotransmitter receptors (De Zeeuw & Hoogland, 2015, Kofuji & Araque, 2021) allowing the cells to detect and respond to neurotransmitter release during synaptic transmission. This is the basis of bi-directional communication between neurons and astrocytes (Figure 1.1) (Araque, et al. 1999; Perea & Araque, 2005).

With astrocytes being non-excitable cells incapable of producing action potentials to communicate, the response to neurotransmitters comes as a product of increased intracellular calcium concentrations (Nedergaard, et al. 2003). Calcium signalling can activate a wide range of downstream processes within the astrocyte, but the key role for bi-directional communication with the neuronal network is the release of gliotransmitters (Figure 1.1). These gliotransmitters are neurotransmitters or neuromodulators released from the astrocyte to feedback to the synaptic network and modulate its strength. Furthermore, the release of gliotransmitters can extend astrocyte signalling to neighbouring astrocytes to initiate similar modulatory mechanisms throughout the syncytium (Araque, et al. 2014).

1.3.1 Receptors Linked to Astrocyte Calcium Signalling

The astrocytes ionotropic and metabotropic receptors monitor synaptic signalling and produce dynamic intracellular calcium transients in response. Ionotropic receptors, including AMPA receptors activated by neuronal release of glutamate, are permeable to calcium ions (David, et al. 1996). Likewise, ATP activation of P2XR have been shown to induce pore formation with movement of calcium ions into and out of the cell (James & Butt, 2002; Chever, et al. 2014).

Ca^{2+} permeable AMPA receptors are particularly seen in Bergmann glia (Nedergaard, et al. 2003; Lalo, et al. 2006), where activation of these receptors has been linked to changes in astrocyte morphology that promote synaptic ensheathment (Iino, et al. 2001; Matsui, et al. 2005; Lippman Bell, et al. 2010). Here ectopic release sites provide a cue for guiding the ensheathment of the synapse to ensure the efficient uptake via astrocyte transmembrane transporters (Iino, et al. 2001; Matsui, et al. 2005).

Metabotropic receptors on the astrocytes elicit downstream signalling by activation of G proteins coupled to the release of calcium from cytosolic stores (James & Butt, 2002). G_q coupled receptors, lead to PLC hydrolysing the membrane lipid phosphatidylinositol 4,5-biphosphate (PIP_2) to diacylglycerol (DAG) and inositol triphosphate (IP_3) which in turn activates the IP_3 receptors of the endoplasmic reticulum releasing Ca^{2+} from internal stores (Kofuji & Araque, 2021). Both mGlu1 and P2Y receptors are G_q-coupled receptors expressed by the astroglia, reacting to glutamate and ATP released by both neurons and astrocytes (Nedergaard, et al. 2003).

1.3.2 Signal propagation

The increase in intracellular calcium initiated by both ionotropic and metabotropic receptors has also been shown to spread in a wave-like formation that propagates throughout the cell to communicate across the large spanning astrocyte syncytium (James & Butt, 2002; Lalo, et al. 2008; Fleischer, et al. 2015). Current evidence suggests that increased intracellular calcium

from an initial stimulus triggers release of gliotransmitters that activates a signalling cascade across local cells creating a wave-like signal (Arcuino, et al. 2002; James & Butt, 2002, Fumagalli, et al. 2003, Fleischer, et al. 2015). Here the calcium response propagates throughout the astrocyte triggered by increasing intracellular concentrations of IP_3 and calcium to mobilise calcium stores throughout and extracellular release of ATP to activate receptors on adjacent cells (Figure 1.2). This 'wave' is observed within the astrocyte when imaged.

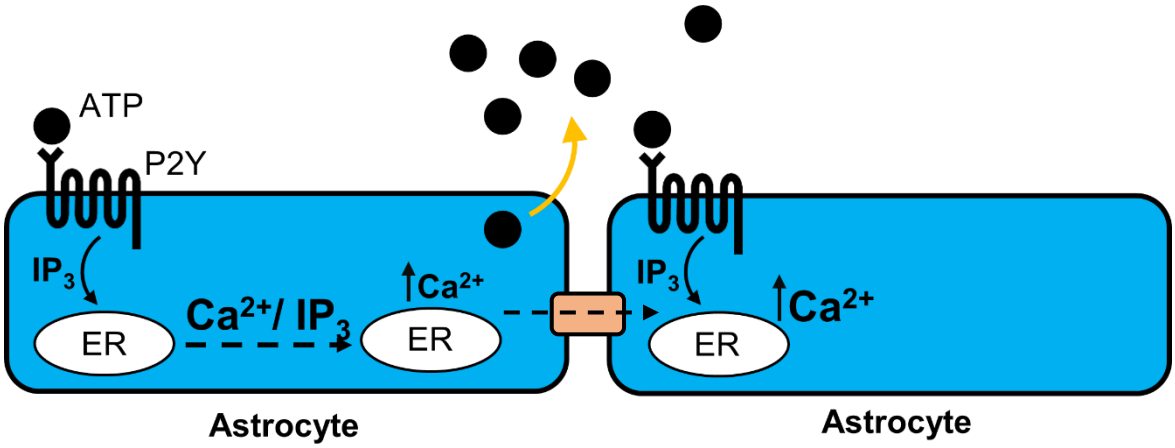

Figure 1.2. Calcium Signal Propagation In Astrocytes. P2Y receptor activation leads to increase in intracellular IP_3 that in turn act on IP_3Rs on the endoplasmic reticulum (ER) to mobilise stores of calcium (Nedergaard, et al. 2003). Increases in intracellular calcium concentrations propagate through the cell soma of the astrocyte and aid IP_3 to further mobilise internal calcium stores from the ER throughout the cell. This is observed as a wave like response. This response can trigger release of gliotransmitters (orange arrow) for a transglial signal as ATP diffuses extracellularly. Astrocyte-astrocyte signalling allows the calcium response to propagate to neighbouring astrocytes observed in fluorescence imaging of astroglia as a 'ripple' effect. Furthermore, transmembrane connexin hemichannels (shown connecting cells) are capable of intracellular exchange of calcium ions and IP_3 for continued propagation of a calcium response (Nedergaard, et al. 2003; Chever, et al. 2014).

Calcium waves therefore spread by both intracellular diffusion of IP_3 and by extracellular paracrine signalling. The release of gliotransmitters from one astrocyte can trigger initiation or potentiation of intracellular increases of calcium through astroglial networks (Bohmbach, et al. 2018). The extracellular component of the Ca^{2+} wave comes most commonly through ATP released either by neighbouring astrocytes or neurons (Arcuino, et al. 2002, Nedergaard, et al. 2003). This acts as a diffusible messenger to activate continued calcium waves throughout the cells via extracellular membrane receptors such as the P2Y and P2X receptors (Hoogland, et al. 2009, Araque, et al. 2014). G-protein coupled P2Y receptors mobilize the intracellular stores of calcium that allow the calcium signal to propagate in a local area – producing a wave-like phenomenon (Nedergaard, et al. 2003). Networks of adjacent astroglia cells allow for cytoplasmic exchange of ions or second messengers that can affect calcium mobilisation from internal stores of astrocytes through various pathways including Cx43 (Connexin-43) hemichannels (Figure 1.2) (Chever, et al. 2014). The amplitude and range of calcium responses within astrocytes can depend on the stimulation type or train and determine whether modulation of synaptic activity occurs locally or spans multiple connected synapses (Araque, et al. 1999; Araque, et al. 2014; Bohmbach, et al. 2018).

Events stimulating local calcium responses, such as AMPA receptors expressed by astroglia, can remain localised in their calcium response. This allows for a homosynaptic modulation affecting structural plasticity and a possible localised release of gliotransmitter at the synapse for signal initiation (Grosche, et al. 2002; Hoogland & Kuhn, 2009; Araque, et al. 2014). A global calcium signal is theorised to come from larger more intense stimuli such as larger stimulus trains or synaptic signal summation and can be associated with P2Y and P2X activation (Araque, et al. 2014). Here, a global astrocyte calcium signal can affect multiple synapses in a heterosynaptic or territorial synaptic modulation path (Araque, et al. 2014). This affects the plasticity of multiple synapses, with the ability to potentiate or depress the neurotransmission having been reported (Nedergaard, et al. 2003; Hoogland et al. 2009; Araque, et al. 2014).

The intricate interactions of astrocytes and glia, with the large diversity of inputs, highlights the complexity of the role they play in neural communication. Neuronal activity and astrocyte inputs are decoded and filtered by the astroglia, allowing for complexity in astrocyte communication. The astrocytes can provide an adaptive feedback and feedforward response that not only supports, but can amplify, the initial input from a synaptic origin. This activity is translated into various spatial or temporal dimensions of calcium response. With this variation, the calcium signalling of astrocytes is an integrated and deeply complex part of their role in brain function.

1.4 Cerebellar Bergmann glia

The spatial range of calcium signalling in astrocytes is the main topic of this project. Previous work in our laboratory has shown that the propagation of calcium signals through Bergmann glial cells of the cerebellum can be altered by distinct patterns of stimulation to the parallel fibres of the cerebellar cortex. The broad aim of this thesis is to investigate the mechanisms that determine the spread of calcium in these specialised astroglial cells.

The cerebellum is the centre for fine motor coordination, receiving and computing the large number of sensory stimuli for refinement of movement, balance and motor learning (Araujo, et al. 2019). More recently, additional associated functions of cognition and learning mechanisms modulate motor learning and sensorimotor integration have been described (Fleming & Hull, 2019; Caligiore, et al. 2019).

The organized laminar structure of the cerebellum comes from the proliferation and migration of cell types through early development and maturation, with observable layers in the transverse plane, of granular, Purkinje and molecular layers. These distinct layers contain functionally different cellular components in differing densities, with highly abundant granule neurons in the granular layer, a single layer of aligned Purkinje neuron somata in the Purkinje cell layer, and relatively low cell density in the molecular layer which is dominated by climbing and parallel fibre inputs to the Purkinje cell dendrites (Hibi & Shimizu, 2012).

Bergmann glia are a distinctive class of astroglial cell that are unique to the cerebellum. Bergmann glia are crucial to the development of the cortical anatomy of the cerebellum, playing a key role in neurogenesis, neuronal growth, synapse formation and cell migration (Araujo, et al. 2019). In the mature cerebellum, the Bergmann glia have a distinct unipolar appearance, with somata in the Purkinje cell layer and elongated fibres that span the molecular

layer of the cortex, terminating in end feet at the pial surface (Figure 1.3A). These Bergmann fibres have multiple protrusions that form leaf like projections, or "microdomains," to surround the synapses in the molecular layer (Figure 1.3B) (Lippman Bell, et al. 2010). This anatomical association with the cerebellar neurons is dynamic, with neurons in culture being able to induce morphological changes and differentiation of the Bergmann glia (Buffo & Rossi, 2013). Three-dimensional reconstructions of Bergmann glia in situ have confirmed this close structural alignment and availability to synaptic transmission, with calcium signals being detected in glial microdomains following synaptic stimulation (Grosche, et al. 2002). This arrangement is an example of a "tripartite synapse" (Perea, et al. 2009).

The enclosure of the synaptic cleft by a Bergmann glial sheath allows for constant communication between synapse and glial cell (Figure 1.3B) (Lippman Bell, et al. 2010; Bellamy, 2006). Excitatory amino acid transporters (EAAT1) on the surface of the Bergmann glia microdomains are involved in the uptake of diffusing extracellular glutamate originating from the presynaptic terminal of the parallel and climbing fibres (Iino, et al. 2001). Furthermore, knockdown of the Bergmann glia AMPA receptors via genetic deletion, or elimination of calcium permeability of the channel by expression of GluA2 subunits, results in profound changes in the morphology and function of the Bergmann glia – with withdrawal of the glial sheath from the synapse, and prolonged kinetics of synaptic transmission at the Purkinje neuron (Iino, et al. 2001; Lippman Bell, et al. 2010).

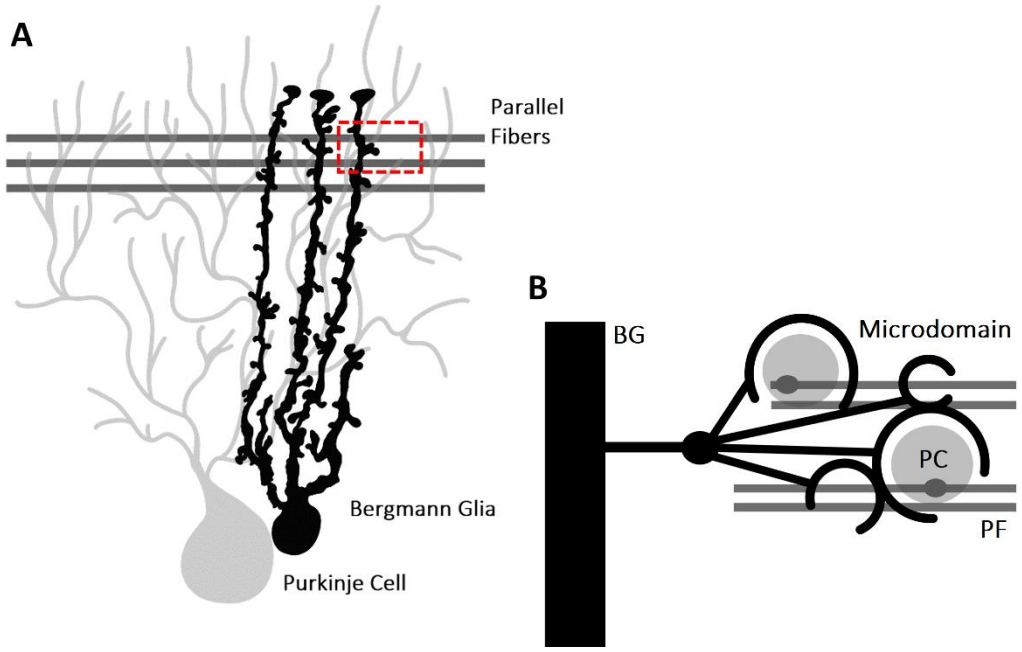

***Figure 1.3. Arrangement of Bergmann Glia in the cerebellar molecular layer*. (A)** Bergmann glial cell here is shown in relation to the Purkinje cell of the molecular layer. The single Bergmann glia shows its unipolar shape with radial fibres extending throughout the molecular layer with end at the pial surface. The Bergmann glia have up to five radial fibres that each show protrusions for neuronal interaction. Each appendage develops small microdomains that enwrap Parallel fibre (PF) and Purkinje cell (PC) synapses providing a compartmentalized unit. **(B)** Cartoon of glial interaction with synapses (red highlighted box). Bergmann glia appendages in abstraction show the leaf like process extend from the cell stem and sheath the neuronal components in a complex pattern (Grosche, et al. 2002) Perisynaptic processes allow proximity of functional components and uptake mechanisms to Purkinje cell and parallel fibre synaptic signalling. The processes enwrap the parallel fibre and Purkinje cell synapses (shown as bulbs) extending through the molecular layer using neuronal signalling as a marker for formation of compartments (Grosche, et al. 2002; Hoogland & Kuhn, 2009). These compartments have been theorised to localise neuronal and glial plasticity (Araque, et al. 2014)

In addition to AMPA receptors, Bergmann glia also express numerous other receptors linked to calcium signalling, including P2X, P2Y, mGlu, H1, ET1, α1 and mACh receptors (Kirishuck, et al. 1996; James and Butt; 2005; De Zeeuw & Hoogland, 2015; Kofuji & Araque, 2021). Stimulation of parallel fibres causes increases in calcium within Bergmann glial microdomains due to activation of AMPA, mGluR and P2Y receptors (Beierlein & Regehr, 2006; Iino, et al. 2001; Piet & Jahr, 2007), with activation occurring from release of synaptic neurotransmitters at ectopic sites outside the active zone of the parallel fibre presynaptic terminal (Dobson and Bellamy, 2015, Dobson, et al. 2018) and Bergmann glia gliotransmitter release (Parpura & Zorec, 2010).

The origin of ATP release in the molecular layer is unclear but has been suggested as a release of gliotransmitters from neighbouring Bergmann glia cells or parallel fibre activation of molecular layer interneurons (Piet & Jahr, 2007; Hoogland, et al. 2009). Bergmann glia offer a target for investigation of how calcium signalling dynamics initiated by neighbouring neuronal elements in a densely organised brain region propagate over long distances along the Bergmann glia network.

1.5 Aims

The overall aim of this project is to investigate the mechanisms that control propagation of calcium signals in astroglial cells. The starting point for the investigation is an unpublished discovery in the laboratory about signal propagation in Bergmann glial cells.

Single-cell recordings of Bergmann glia in acutely isolated cerebellar slices (transverse section, Wistar rat, aged 16-20 days postnatal) show that stimulation of parallel fibres in the molecular layer leads to calcium signals that propagate from the microdomains surrounding the synapses along the Bergmann fibres and to the cell soma (Figure 1.3). The spatial range of the calcium response depends on stimulation frequency and intensity, with an optimal calcium response observed with a train of 10 pulses at 30 Hz (Figure 1.4B, C). Further investigation revealed that a specific stimulation protocol that induces long-term potentiation (LTP) at the parallel fibre Purkinje cell synapse (16 Hz for 15 s; see Dobson & Bellamy, 2015) causes the opposite effect – long-term depression – of the spatial range of the calcium signal in adjacent Bergmann glia (Figure 1.4E, F).

The mechanism of this long-lasting reduction in the spread of calcium signal is unknown, but it suggests that the range of astroglial calcium spread can be modulated by particular patterns of stimulation. Preliminary pharmacological experiments have indicated that the known modulatory receptors at the parallel fibre synapse that can alter neuron-glial transmission (Dobson & Bellamy, 2015) are not responsible for the depression of calcium signal propagation (unpublished data).

The objectives of this project are to advance understanding of calcium propagation in astroglia in three ways:

1) To use cultured astrocytes to investigate whether autocrine/paracrine release of ATP contributes to calcium responses to glutamate at early and late periods of stimulation, and to identify the purinoreceptors that may be involved.

2) To develop a method for bulk loading of calcium indicator into Bergmann glial cells in cerebellar slices, to allow for imaging of signal propagation throughout the molecular layer.

3) To test whether serotonin may play a role in the spatial plasticity mechanism that alters calcium propagation in Bergmann glia.

Success in these aims would improve our understanding of the P2 receptor types involved in calcium wave propagation in astroglia in culture and in situ, provide a less technically demanding method of measuring Bergmann glial calcium responses (compared to patch-clamp electrophysiology), and test the hypothesis that serotonin inputs to the cerebellum may play a role in regulating the spatial range of glial calcium signalling.

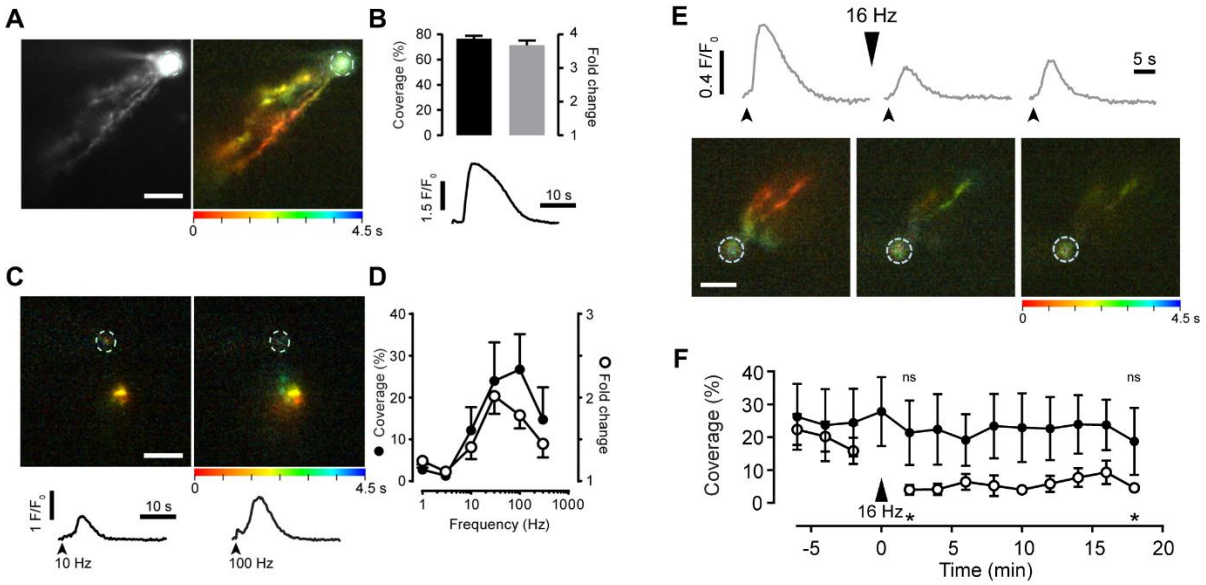

Figure 1.4. Spatial plasticity in calcium signal propagation in Bergmann glial cells. **(A)** Epifluorescence image of a Bergmann glial cell in an acutely isolated slice of rat cerebellum (Wistar, 18 days postnatal). The cell was loaded with the calcium indicator Fluo-5F (100 µM) during whole-cell patch clamp recording and stimulated with puff application of 1 mM ATP to the molecular layer. Calcium response is shown as greyscale maximum intensity projection (left) and as a spatiotemporal projection pseudo-coloured for time after stimulation (right), to illustrate propagation of the signal along the radial fibres from site of initiation. (Scale bar = 25 µm); dashed outlines indicate soma position. **(B)** Calcium response to ATP puff quantified as spatial range (percent coverage of region of interest that encloses glial arborescence) and fold change response (normalized to pre-stimulus fluorescence intensity). Data are mean ± SEM for 5 cells averaged over three consecutive stimuli. Below: representative trace of mean calcium response recorded in glial arborescence ROI. **(C)** Spatiotemporal and fold change responses of a glial cell response to parallel fibre stimulation in the molecular layer (100 µA, 80 µs) at 10 Hz (left) and 100 Hz (right). **(D)** Mean percentage coverage (solid circles) and fold change (open circles) of arborescence response against stimulation frequency (10 pulses at 75-100 µA) (n=8-10 cells). **(E)** Fold change responses during repeated stimulation (every 2 min) of parallel fibres in bursts that cause widespread calcium propagation through glial arborescence (30 Hz, 10 pulses, 50-100 µA). Traces are the mean of three consecutive trains delivered to a single cell before (-7 to -2 min), and after (2-8 min and 14-18 min) induction of synaptic long-term potentiation with a 16 Hz, 15 s tetanus. Spatiotemporal maps below are matched to these time points. Note long-lasting reduction in the spatial range and mean fold change of the calcium response because of LTP induction. **(F)** Aggregate data showing the mean percent coverage of calcium response in control cells (filled circles, no 16 Hz tetanus) and in cells receiving 16 Hz stimulation (at arrow; open circles). Statistical significance was tested using one-sample t-tests at individual time points relative to mean control values (ns, *P*=>0.05) (*, *P*=<0.0001). Data are mean ± SEM of 10 and 11 cells, respectively.

All experiments and analysis conducted by Dr Katharine Dobson, University of Nottingham.

2 Materials and Methods

2.1 Ethics

All experiments and animal use within the duration of this study were performed within the guidelines and code of practice outlined by the British Home Office Animals (Scientific Procedures) Act (ASPA) 1986 and the University of Nottingham Animal Welfare and Ethical Review Board. All tissue collection experiments were performed in accordance with Schedule 1 of ASPA ascertaining to the humane killing of animals by a competent individual.

2.2 Cortical Astrocyte Cell Culture

Cell culture preparation was carried out by Dr Rawan Hareeri on a routine basis for preparation of plates used within this study, as previously described (James, et al. 2011).

Briefly, neonatal (P1-2) Wistar rats were humanely killed by cervical dislocation and decapitated before dissection of the brain. The whole cortex was removed and then maintained in dissection buffer (Hanks Buffer solution, pH 7.2) in sterile conditions in a flow hood. The tissue was chopped with a razorblade before being mixed with glial medium (450ml Dulbecco's modified eagle medium (DMEM), 50ml Foetal Bovine Serum (FBS), 4500mg/l glucose, 4 mM L-glutamine, 110 mg L-pyruvate, 50 µg/ml L-proline, 100 units/ml penicillin and 100 µg/ml streptomycin) and papain. The solution containing tissue was incubated for 40min at 37°C. DNase is added to the dissociated tissue in suspension and spun in centrifuge, supernatant is removed and discarded. A series of trituration and centrifugation procedures are performed, with the collection of supernatants containing dissociated cells in glial medium.

The cell suspension was then strained through 100 µm cut off cell strainer and the cell count density were measured using a haemocytometer. Final cell density of $1x10^6$ is measured and solution and glial medium placed in 6 well plates for 2 weeks before cell splitting onto poly-l-lysine coated coverslips – in which experiments are performed 48hrs later. Plates are maintained for the maximum time of a further week and used within this time, preferably between 48-72hrs of splitting.

2.3 Ca^{2+} Cell Imaging

Astrocytes adhered to coverslips were maintained in glial medium in six well plates that were kept in an incubator. Coverslips with adherent astrocytes were transferred from plates into a small petri dish containing room temperature HEPES Buffered solution containing (mM); NaCl (135), KCl (3), HEPES (10), glucose (15), $MgSO_4$ (1), $CaCl_2$ (2). Coverslips were incubated with 1 µM of Ca^{2+} indicator Fluo-5F AM in 20% Pluronic for 30 minutes total, while protected from light. Coverslips were then transferred to a dish containing only HEPES Buffer and further left for a period of 30 minutes to allow de-esterification of the indicator.

The prepared coverslip was transferred into an imaging chamber and mounted on the stage of a Brunel Ltd SP-98-FL inverted fluorescence microscope (Brunel Microscopes Ltd) with

connecting Hamamatusu C4742-95 ORCA-ER digital camera (Hamamatusu Photonics). Fluorescence excitation 480 nm wavelength was carried out with a Cool LED pE-100 light source. Emitted light was collected through a bandwidth filter of 535/45 nm. Images were acquired with software (Micro-Manager 1.4) with a protocol for detection of exposure time of 250ms, acquired at frame a second for a total of 1200s (20 minutes).

Coverslips are maintained in buffer at room temperature, with presence of vacuum line to the surface of the bathing medium to allow for bulk solution exchange. Pharmacological agents were applied by bulk displacement of bathing solution. In instances of antagonists and blocking compounds, antagonist was added when the coverslip was transferred to the imaging chamber and left for at least 2-5 minutes before the start of the imaging experiments.

2.4 Image Analysis of Cortical Astrocyte

Data collected from cortical astrocytes was processed in frame stack format and analysed using ImageJ time-series analyser V3 plugin. Mean grey value of regions of interest centred on cells was used as a parameter for quantifying changes in fluorescence intensity of each cell.

The fluorescence is quantified as the ratio of F/F_0 in which F_0 is the mean value of the first 25 s of recording. The data is processed using MathWorks MATLAB 2019 with a custom-written Calcium imaging GUI. This configuration is selected to the frames spanning from addition of agonist (120 frame) for 80 following frames (until 200 frame) to segment the response for addition of agonist and determine a direct cell response. A cell is determined to have been 'responsive' if the value of its mean F/F_0 is increased above the threshold of 3 times the standard deviation of the value before agonist was added. Initial responses were quantified as the percentage of cells per coverslip that responded, and the maximum fold change observed for responding cells in the initial stimulation period. "Late-stage" signalling was analysed as AUC (F/F_0 / s) of all cells for the final 300 frames and analysed as individual cells. Parameters produced by MATLAB Calcium GUI were tested for statistical significance within PRISM GraphPad 7.04. Coverslips or specific cells were manually excluded from analysis if cell imaging was compromised with external errors (including frame shift, presence of dust or unadhered cells).

2.5 Tissue Slice Preparation

Wistar Rats (P16-20) of either sex were humanely killed by cervical dislocation and decapitation and the cerebellum removed rapidly and maintained in Krebs Buffer containing (mM): NaCl (125), KCl (3), NaH_2PO_4 (1.5), $NaHCO_3$ (25), glucose (15), with 3mM $MgSO_4$ kept on ice and aerated with carbogen 95% O_2 / 5% CO_2. The cerebellum was then cleaned of meninges and visible surface blood vessels, before being secured to the base disc of a vibratome with cyanoacrylate adhesive at the base. The cerebellum was continually aerated and kept in chilled Krebs buffer (containing 3mM $MgSO_4$) within a vibrating microtome (Leica Vibratome). 300µm transverse slices were prepared and transferred to a recovery chamber in Krebs buffer (2mM $CaCl_2$, 2mM $MgSO_4$) at 32°C for 1 hour with continual bubbling by carbogen, followed by cooling for an additional 30 minutes to room temperature.

Slices were transferred into a built-in chamber of an upright fluorescence microscope rig (Nikon E600FN) and perfused with carbogenated Krebs Buffer (2mM $CaCl_2$, 1mM $MgSO_4$) to create a maintained bath solution with slice. Slices were held with a weighted nylon mesh against the base of glass chamber and live imaged using x60 Fluor lens (Nikon Japan).

Borosilicate stimulating electrodes were fashioned and loaded internally with 100 µM Fluo-5F AM in Pluronic in Krebs Buffer (2mM $CaCl_2$, 1mM $MgSO_4$) and positioned within the molecular layer of slices with applied positive pressure and left for 30 minutes in dark room laboratory. Following extracellular loading, imaging was carried out using a standard FITC filter set, and HCImage Live software. Images were acquired for a total of 100 frames of a total 30 seconds per data file and each stimulus, with a computer assisted triggering of a Hamamatsu C1440 Digital Camera (Hamamatsu Photonics), and Cool LED pE100 excitation light source.

2.6 Electrophysiology

Application of stimuli at 30 Hz and 16 Hz were carried out with a constant-current isolated stimulator at 100 µA for 80 µs. Bulk loading of calcium indicator was via the stimulating electrode internal solution which contained Fluo-5F AM in Krebs Buffer (2 mM $CaCl_2$, 1 mM $MgSO_4$).

30Hz stimulation is delivered as 10 pulses over 300 ms following 1000 ms of recording, followed by continued image recording of tissue for the remainder of time for a total of 30 s with frame rate of 3.33 fps. 16 Hz stimulation is delivered with 240 pulses over 15 s following 1000 ms of recording and continues recorded imaging for the remainder of 30 s.

In the cases of antagonist or blocking compounds a solution was prepared in Krebs Buffer (2mM $CaCl_2$, 1mM $MgSO_4$), and also carbogenated. The solution was perfused into the imaging bath immediately following the second tetanus and continues over a 10-minute period to fully displace the buffer. A third tetanus is performed in antagonist solution.

2.7 Image Analysis of Tissue Slices

Data Stacks of 100 frames each were processed using ImageJ with Time Series Analyzer V3. Each data stack is processed by removal of an average Z project of the first 3 frames of each stack that are subtracted from the original data stack – this produces a background subtraction of the data allowing for observation of only fluorescence change (ΔF).

Manually a ROI is produced identifying the Bergmann fibres via morphological identification and orientation in slice using the location of molecular and granular layers and the high amplitude fluorescence response of the parallel fibre bundle during stimulation. This ROI aims to isolate visible fluorescence perpendicular to parallel fibre signal (the orientation expected for Bergmann fibres), as a visual cue for manual determination of ROI. However, due to the overlapping nature of the molecular layer components, some parallel fibre fluorescence signal is inevitably present within the ROI measured. The mean grey value was measured per frame and plotted against the frame number to complete a trace for each data stack.

Data was quantified as Area Under the Curve (AUC) for the fluorescence change during the post-stimulus period, beginning at the first frame following stimulation conclusion. The effect

of pharmacological and 16 Hz treatment was assessed by normalising AUC after treatment to before treatment, as described in chapter 4.

3 Cortical Astrocytes In Cell Culture

3.1 Introduction

Astrocyte responses to neurotransmitter release involve propagation of intracellular calcium waves throughout the astrocyte and through networks of connected cells (James and Butt, 2002). These calcium waves within astrocytes were initially characterised by Cornell-Bell, et al. 1990 and further explored by Guthrie, et al. 1999 who highlighted extracellular ATP as a source to both initiate and propagate intracellular calcium waves.

ATP can originate from both excitatory neurons and interneurons but can also come from astrocytic gliotransmitter release during astrocyte-astrocyte signalling (Fumagalli, et al. 2003). ATP release as a gliotransmitter can result from the signalling cascade of calcium intracellularly, triggered from activation of P2 purinergic receptors in an autocrine/paracrine fashion. Evidence has shown the expression of P2 receptors on astrocytes; both metabotropic P2Y and ionotropic P2X receptors, in which cultured astrocytes have displayed increased intracellular calcium following activation by selective agonists (James & Butt, 2002; Lalo, et al. 2008).

P2Y purinoreceptors are G protein coupled receptors (G_q) that increase intracellular inositol trisphosphate (IP_3) and trigger release of Ca^{2+} from internal cellular stores - a cascade which initiates a calcium wave and a 'ripple effect' that propagates through the cell cytoplasm and into neighbouring cells via gap junctions (James & Butt, 2002; Lalo, et al. 2008; Fleischer, et al. 2015).

P2X receptors are calcium permeable ion channels. $P2X_7$ receptor activation after prolonged exposure to ATP and stimulation also allows for calcium wave propagation in astroglia (James & Butt, 2002; Lalo, et al. 2008; Fleischer, et al. 2015; Svobodova, et al. 2018). The $P2X_7$ receptors form transmembrane pores allowing for the influx of extracellular calcium to elicit calcium waves intracellularly, which can reliably be blocked with removal of calcium from the extracellular buffer (Fumagalli, et al. 2003). However, the $P2X_7$ pore appears primarily responsible for a small part of the calcium signal in astrocytes in comparison to the $P2Y_1$ receptors (Fumagalli, et al. 2003).

Intracellular calcium increases are further amplified with calcium ion dependent activation of endoplasmic reticulum calcium channels. These channels are ryanodine receptors (RyR) and IP_3 receptors, activated by calcium influx and initial IP_3-receptor calcium release propagates the wave in a mechanism of calcium induced calcium release (CICR) (Parpura, et al. 2011). This mechanism arises from cooperativity of binding, where calcium binding to individual sites on the ryanodine and IP_3 receptors increases the affinity for adjacent binding sites. This has the effect of increasing the probability of channel opening, amplifying local calcium concentrations (Lanner, et al. 2010). This mechanism allows for subcellular calcium transients to spread by triggering the opening of neighbouring channels, causing the wave to propagate intracellularly in the astrocyte (Croft, et al. 2016).

Further study has highlighted the mechanisms for calcium wave propagation in astrocyte cultures, with current evidence suggesting a combined extracellular component due to release

of ATP from astrocytes to activate P2X and P2Y receptors in neighbouring cells (James & Butt, 2002, Fumagalli, et al. 2003, Fleischer, et al. 2015), and an intracellular component via diffusion of calcium and IP_3 through gap junctions (Fleischer, et al. 2015; Svobodova, et al. 2018).

Neuronal release of glutamate from the synapse or from astrocyte specific release sites can also trigger astrocyte calcium responses (Parpura & Zorec, 2010). Here glutamate can act through ionotropic AMPA or metabotropic mGlu receptors for increases in intracellular calcium (Nedergaard, et al. 2003; Pangršič, et al. 2007). Glutamatergic stimulation of astrocytes has been shown to trigger the quantal release of ATP from cortical astrocytes through exocytosis mechanisms (Pangršič, et al. 2007), indicating that the initial calcium response to glutamate receptor activation could be amplified and prolonged by secondary ATP signalling.

3.1.1 Blocking of P2 Purinergic System

Previous work in this laboratory has shown that pharmacological blockade of both P2Y and P2X receptors present on cortical astrocytes inhibited the increase in calcium concentrations and burst spikes of Ca^{2+} caused by ATP (James, et al. 2011) – indicating that both ionotropic and metabotropic purinoceptors are expressed under our culture conditions.

Other literature supports these results with evidence of P2Y and P2X presence - possessing a broad spectrum of P2 subtypes, with expression for $P2Y_1$, $P2Y_2$, $P2Y_4$, $P2Y_6$, $P2X_{1\text{-}5}$ and $P2X_7$ (James & Butt, 2002; Fumagalli, et al. 2003). Calcium signal propagation is dependent on specific P2 receptor subtypes, with the primary involvement of the $P2Y_1$ and $P2X_7$ receptors, in which in cultured astrocytes have shown intracellular calcium oscillations to be decreased in the presence of non-selective antagonists, including PPADS and suramin (Fumagalli, et al. 2003). Astrocyte release of ATP as a gliotransmitter is also successfully blocked by negative allosteric modulators and potent antagonists of $P2Y_1$ and $P2X_7$ receptors in a concentration dependent manner (Svobodova, et al. 2018)

Previous research had found success in the use of PPADS as a broad-spectrum blocker of astrocyte purinergic receptors. PPADS is widely reported to be successful in blocking of purinergic P2 receptors for astrocytes (James & Butt, 2002), with reported dose dependent manner, and with similar effects on rat variant $P2X_4$, $P2X_7$ and $P2X_2$ receptors (Fleischer, et al. 2015). Additionally, evidence reports the antagonistic effects of PPADS in blocking the ATP and 2-MESADP ($P2Y_1$, $P2Y_{12}$ & $P2Y_{13}$ agonist) activation of P2Y receptors, with greater efficiency with $P2Y_1$ receptor subtype (Jacob, et al. 2014). Similarly, suramin is an additional broad spectrum P2 receptor antagonist, which has previously shown $P2Y_1$, $P2X_4$, $P2X_5$ and $P2X_7$ sensitivity (Guthrie, et al. 1999; Beamer, et al. 2017).

The goal of this first stage of the project was to assess the extent to which autocrine and paracrine ATP release from astrocytes contributes to propagation of observed wide-ranging calcium signals. First, the initial response of the astrocytes to glutamate is measured in the presence and absence of a broad-spectrum antagonist to purinoreceptors to establish whether the large-scale calcium mobilisation through cultured astrocytes triggered by glutamate also depends in part on extracellular ATP release. Next, the late stage of the glutamate response, when equilibrium has been established, is compared to determine whether ATP signalling reinforces or prolongs the response to glutamate.

Finally, experiments were used to identify the receptor classes contributing to ATP-induced calcium responses in these cells and test the effectiveness of the broad-spectrum antagonists for blocking signal propagation from ATP. In addition to testing these broad-spectrum antagonists, we also assessed the impact of blocking P2Y and P2X subtypes using a $P2Y_1$ selective antagonist MRS2179 (Fumagalli, et al. 2003; Jacob, et al. 2014; Svobodova, et al. 2018) and a P2X-selective antagonist TNP-ATP (Lalo, et al 2008; Ikeda, et al. 2012).

These experiments were designed to better understand the role of ATP release in amplifying and prolonging calcium signals initiated by glutamate, and hopefully identifying pharmacological agents that can be used to examine spatial plasticity and signal propagation of astroglia in cerebellar slices.

3.2 METHODS

Preparation of cortical astrocyte cell culture can be referred to in in section 2.2-4.

Astrocytes were loaded with Fluo-5F AM (1 µM) in HEPES buffered saline solution for 30 minutes with a following 30-minute de-esterification period, all performed in minimum light exposure. Coverslips of cells were mounted into a silicone grease sealed imaging chamber, bathed in buffer, then transferred to the stage of the microscope. A vacuum line was positioned near to the surface of the solution, and cells then brought into focus using the brightfield of the microscope for a minimum time due to photosensitivity.

Pharmacological solutions were prepared on the day of experiment and stored on ice as stock solutions before dilution into buffer immediately before addition. ATP (10 µM) and glutamate (100 µM) were added to the cells within the imaging stage at 120s, by displacement of the solution within bath (~5 ml).

In instances of antagonist pharmacological investigation, the antagonists were applied to the cortical astrocytes directly following transfer to the microscope stage (approximately 3 minutes before experiments begin). ATP (10 µM) or glutamate (100 µM) were coapplied with antagonist in HEPES buffer.

Final concentrations were as follows; PPADS (100 µM), suramin (100 µM), MRS2179 (20 µM), TNP-ATP (1 µM). All drugs ordered and supplied through Tocris (bio-techne).

Imaging and analysis of images performed is as described in Section 2.3-4. From each coverslip every individual cell that is visible is assigned an ROI and analysed for maximal response amplitude and for area under curve at a late stage of stimulation. The percentage of cells responding for each coverslip was also calculated, with a response defined as any cell that has an increased in fold change fluorescence >3 SD greater than baseline variation.

Measurements have been demarcated into the initial response of quiescent astrocytes to the immediate addition of glutamate or ATP, analysing an 80 second period from frame 120-200, and a late phase response, measured for each cell from frame 900-1200 for a total of 300 frames (Figure 3.1). For AUC, a value of 300 (300 s x 1 F/F_0) is subtracted from the values in order to remove baseline area (dashed line in corresponding figures).

One-way ANOVA is used to compare the percentage of cells responding per coverslip. The maximum fold change of the initial fluorescence response and the late-stage response displayed as under the curve (AUC) is compared using the non-parametric Kruskal-Wallis test as data was not normally distributed (assessed by D'Agostino-Pearson test). All tests were carried out in GraphPad Prism.

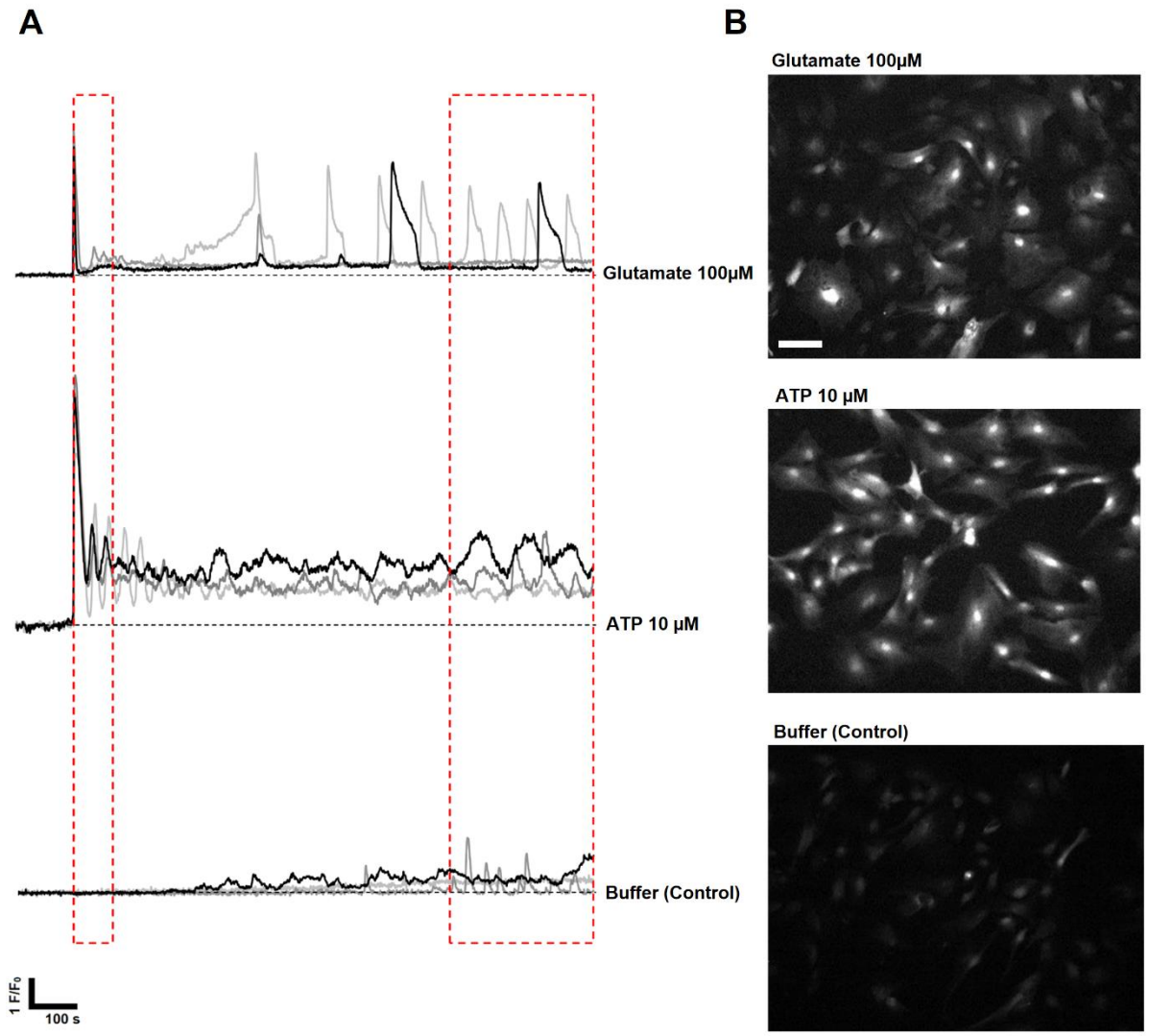

Figure 3.1. Calcium Response Analysis In Cultured Cortical Astrocytes. (A) Fluorescence traces of single cell ROIs displaying F/F_0 over time for the full 1200s protocol. Each trace is representative of a single ROI centred on an individual cell. Here 3 examples of each response are shown that are representative of the average response for glutamate (100 µM), ATP (10 µM) and a control buffer (as indicated). Agonist or buffer were added by solution exchange after 120 s. The initial response is analysed from frame of application (120s) to frame 200s to isolate a calcium response (indicated by first red box). This allows analysis of an initial response for both glutamatergic and purinergic signalling pathways. For this initial response the % of cells responding per coverslip was tested, and max F/F_0 change of all responding cells is also calculated. A late phase response to investigate calcium wave regeneration and propagation is analysed for 300s between frames 900-1200. This later phase is analysed as AUC $((F/F_0)/(s))$ to assess total calcium flux in this period. **(B)** Example images of loaded cells are shown from matching traces in (A), each 3 traces represent 3 cells that appear in images in B. (Scale bar = 50 µm). Frame is taken from the initial response period (120-200) to indicate the calcium response in relation to glutamate, ATP and Buffer.

3.3 RESULTS

This investigation began in identifying if there is a purinergic component to calcium signalling and calcium wave propagation in astrocytes triggered by glutamate.

Initial stimulation of the astrocytes with glutamate shows a significant increase in cells exhibiting a calcium response after solution exchange, rising from 16.9% in control to 66.9% with glutamate (Figure 3.2). This response is consistent with the presence of AMPA receptors and mGluR1 receptors expressed by the astrocytes (David, et al. 1996; Lalo, et al. 2006; James, et al. 2011) (Figure 3.2A)

Control experiments using exchange of buffer solution in an identical protocol still presents a small number of cells responding in this time window, highlighting some constitutive activity of the astrocytes in culture (Figure 3.1A, 3.2).

PPADS, a broad-spectrum antagonist of purinergic receptors, failed to significantly reduce the number of responding cells in the presence of glutamate or after buffer exchange control (Figure 3.2B). Although data shows a decrease in mean percentage of cells responding it is not statistically significant (ns, P=0.8178 vs Glu). Furthermore, there is no significant decrease of the fluorescence fold change max of individual cells in response to glutamate when PPADS is applied in responding cells (Figure 3.2C). This would suggest that the initial large calcium response observed in cortical astrocytes does not have a purinergic component that is sensitive to PPADS.

Next, we tested whether late-stage calcium response following prolonged stimulation may have a PPADS-sensitive component. In all conditions, calcium increases above baseline can be observed in the final 5 min of experimentation (Figure 3.3A), indicating that even astrocytes in standard imaging buffer show some spontaneous activity. The AUC during this period was highly variable between cells (Figure 3.3C) and a test for normality indicated that these population responses were not normally distributed (P=<0.0001 by D'Agostino-Pearson test).

Addition of glutamate did not significantly increase the AUC of calcium signalling compared to control or PPADS alone (Figure 3.3B, P=>0.9999) Counterintuitively, pre-treatment with PPADS significantly increased the area under the curve of fluorescence changes in cells stimulated with glutamate during this late period (****, P=<0.0001 vs Glu) (Figure 3.3B).

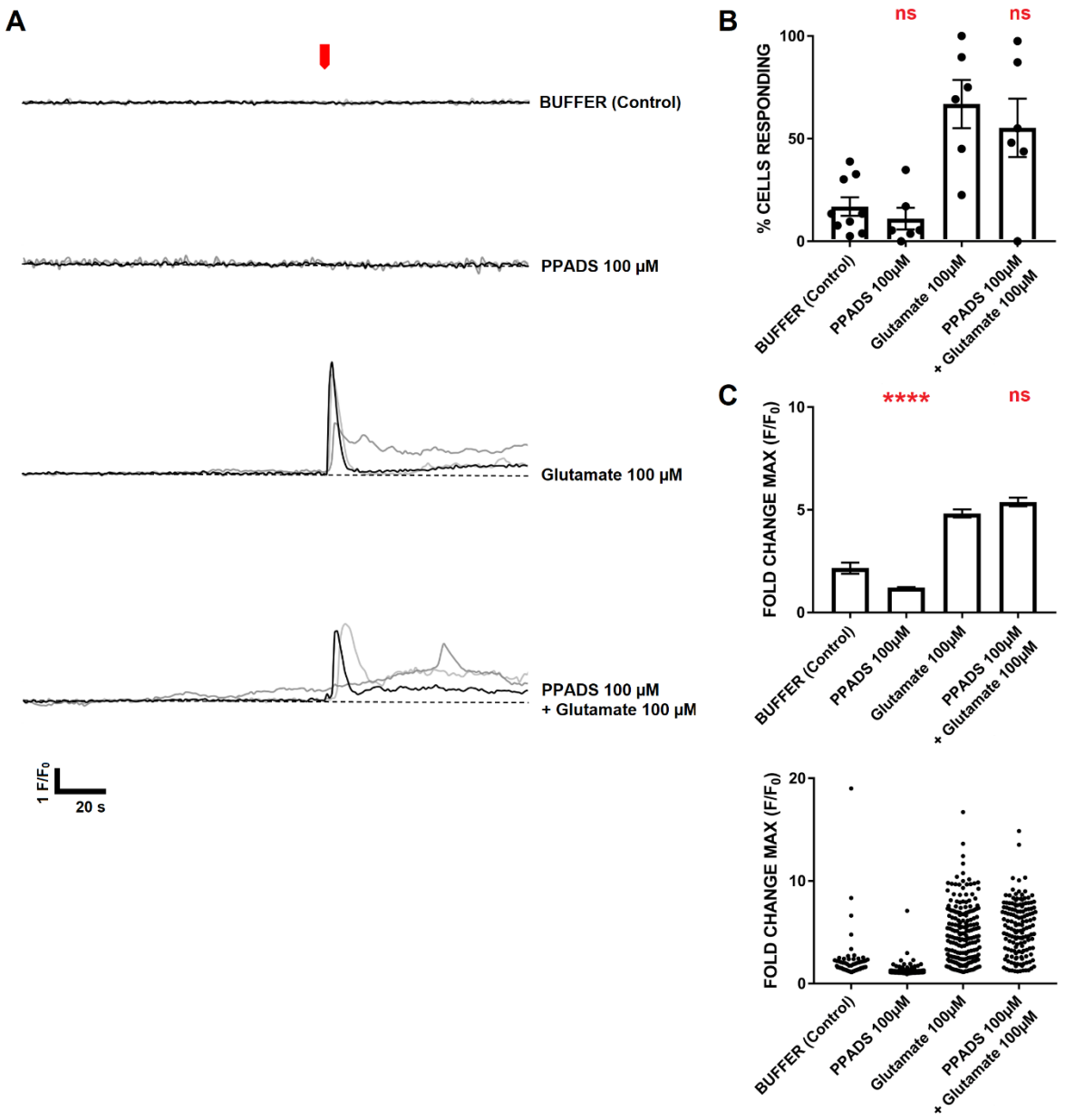

Figure 3.2. Calcium Signalling In Cortical Astrocyte Cell Culture In Response To Glutamate. (A) Fluorescence traces of single cell ROIs displaying F/F_0 over time, during exposure to PPADS (100 µM), glutamate (100 µM), and glutamate + PPADS (100µM) for initial response period. Application of drug or buffer (marked as red arrow) occurs at 120s from start of recording. Each example trace represents individual cell ROIs identified from image (dashed line indicates 1 F/F_0). **(B)** % of cells responding per coverslip measured as F/F_0 increasing above threshold of 3 SD over baseline variation before addition, with a window of 80s from 120s-200s to measure, Buffer (n=9) shows some spontaneous activity, and application of PPADS does not affect this (ns, P=0.9914 vs Buffer). Glutamate (Glu) (100µM) (n=6) shows marked increases in calcium signalling which is not significantly blocked by PPADS (100µM) (n=6, P=0.8178 vs Glu). **(C)** Fold change Max (F/F_0) of responding cells shown as mean ± SEM (top) and of each individual cell analysed (bottom). There are no significant changes in fluorescence response in the presence of PPADS compared to glutamate (ns, P=0.575) but does significantly affect spontaneous responses in buffer (****, P=<0.0001).

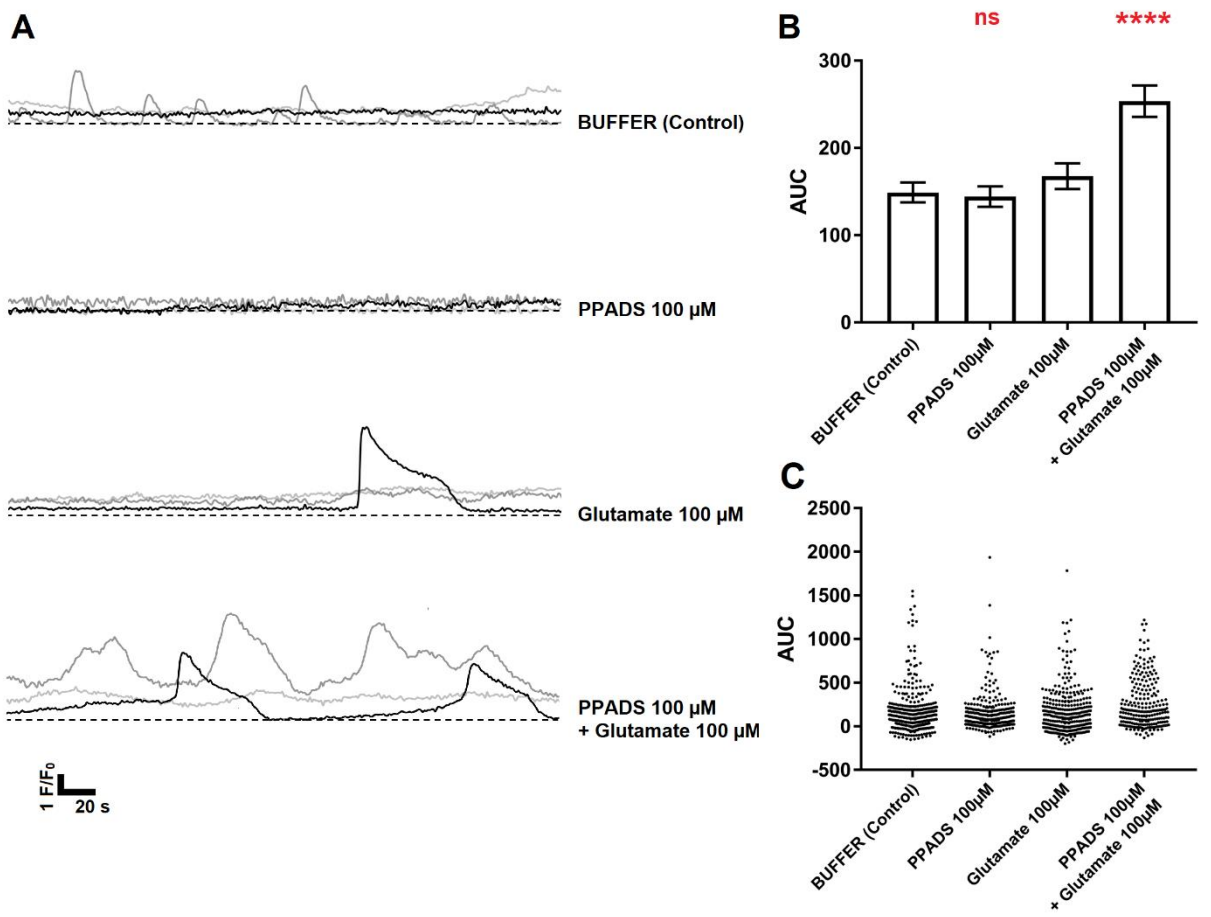

Figure 3.3. Late-Stage Calcium Signalling in Cortical Astrocyte Cell Culture in Response to Glutamate. (A) Fluorescence traces of single cell ROIs displaying F/F_0 over time, during exposure to PPADS (100 µM), glutamate (100 µM), and glutamate + PPADS (100µM) for time period of analysis for late-stage response, traces show 900s to 1200s. Each example trace represents individual cell ROI identified from image (dashed line indicates 1 F/F_0). Traces are selected as a representation of mean data and only shows 3 individual cell responses each. **(B)** AUC ($(F/F_0)/(s)$) with a background subtraction is analysed for 300 frames (900-1200s) to determine calcium signal propagation and regeneration in the cortical astrocytes over a longer period. Here there is a significant increase in late-stage calcium response of glutamate (n=6) (n=coverslips) and the addition of PPADS with glutamate (n=6) (****, P= <0.0001 vs Glu). Also, PPADS has no effect on any spontaneous activity seen within buffer solution (ns, P=>0.9999 vs Buffer). **(C)** AUC of each individual cell displays the large variance of the responses observed when totalled from each coverslip, data shown to not to be normally distributed (P=<0.0001). Some cells drop below the baseline response of 0, this represents cells where fluorescence declines below the baseline at the start of the experiment.

These results prompted us to directly identify the purinergic receptors expressed in the cultured cells, by testing broad-spectrum and isoform selective antagonists for P2 receptors. The addition of 10 µM ATP to the astrocytes provoked a mean of 99.7% of cells responding in the early phase. This response was significantly greater than that of glutamate on the cultured cortical astrocytes (P=0.0016). Unlike that of the glutamate, ATP stimulus is significantly reduced by PPADS in astrocytes, to 69.1% (**, P=0.0080 vs ATP) (Figure 3.4A, B).

An alternative non-specific P2 purinergic antagonist, suramin, revealed a much more substantial block of astrocyte responses, with only 25% (****, P=<0.0001 vs ATP) of the cells responding to ATP in the presence of suramin. The inhibitory effect of the suramin brought the % of cells responding down towards the level of the control buffer data (Figure 3.2B). Both PPADS and suramin show significant decreases in their fold change max in response to ATP (****, P=<0.0001) (Figure 3.2C).

Selective antagonists for the ionotropic and metabotropic subtypes that are encompassed within P2 purinergic receptors were used to try and isolate possible specific subtypes involvement. The metabotropic P2Y1 receptor antagonist MRS2179 (Jacob, et al. 2014), failed to reduce the ATP induced calcium signalling for cells responding (ns, P=0.8631 vs ATP) (Figure 3.4B). Furthermore, a selective antagonist for P2X, TNP-ATP (1µM) also failed to show any specific inhibitory effect on the cells responding to ATP in a calcium related manner (ns, P=>0.9999 vs ATP), suggesting that neither receptor class is solely responsible for the observed responses. MRS2179 showed significant decreases in the fold change max of responding cells, while TNP-ATP did not (Figure 3.3C).

Next, late-stage calcium signal response was investigated to determine if the alternative antagonists could block these ongoing responses (Figure 3.5). Broad spectrum blocking using PPADS does not affect the late-stage calcium response (ns, P=>0.0999 vs ATP). In contrast, the broad-spectrum antagonist suramin significantly decreases the calcium response at this timescale (****, P=<0.0001 vs ATP). Suramin also decreased calcium response below the level of buffer control (Figure 3.5B).

The effect of selective P2 antagonists had mixed effects during the late stage response. P2Y1 receptor antagonist showed a significant increase in AUC following initial ATP stimulation (****, P=<0.0001 vs ATP), similar to that observed for PPDAS in the presence of glutamate (Figure 3.3). P2X specific antagonist, TNP-ATP, however had no significant effect (P=0.0781).

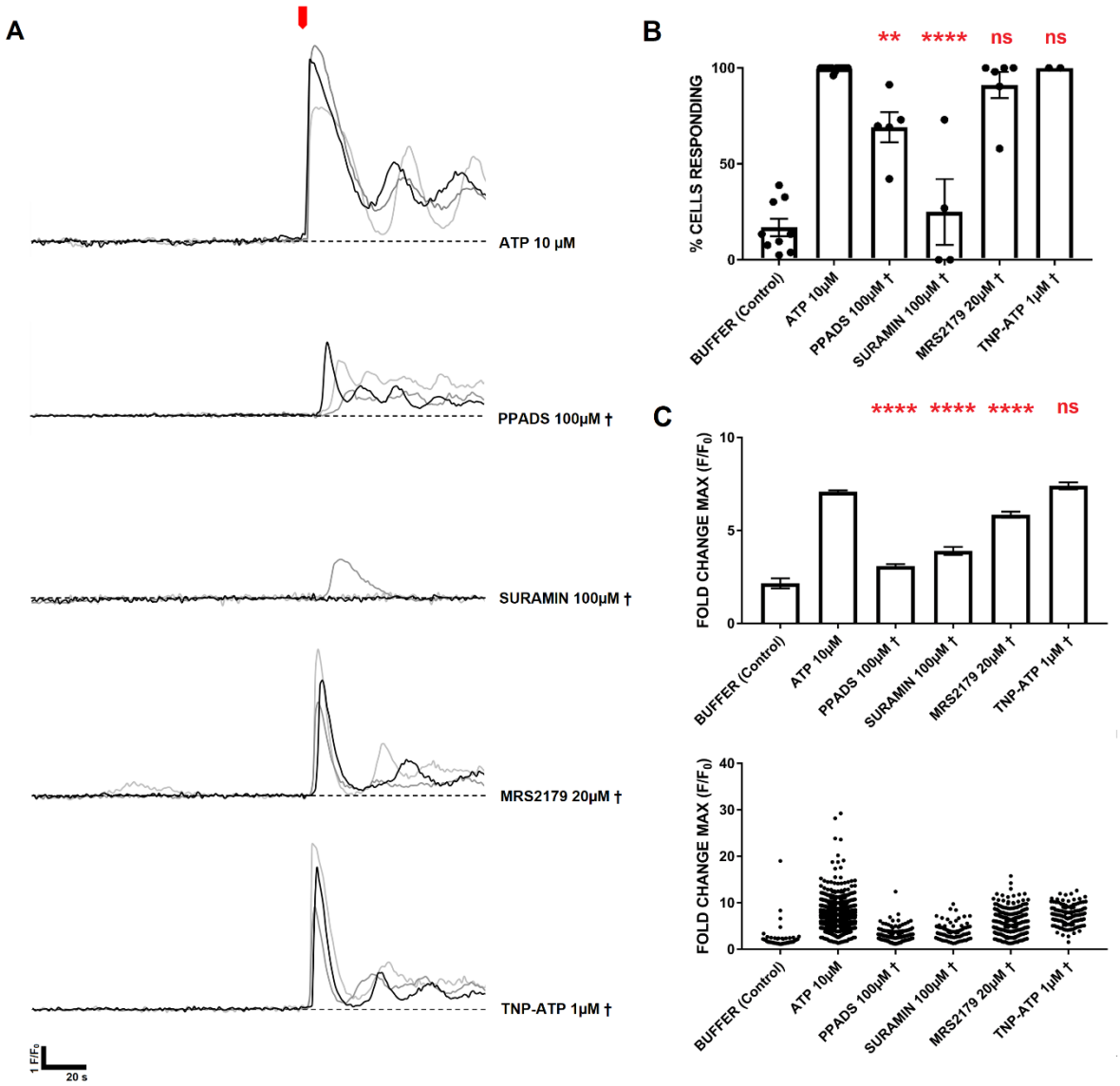

Figure 3.4. Calcium Signalling in Cortical Astrocyte Cell Culture in Response to ATP (A) Fluorescence traces of single cell ROIs displaying F/F_0 over time during exposure to ATP (10µM), PPADS (100µM) † and suramin (100µM) †, TNP-ATP (1µM) † and MRS2179 (20µM) †, for time period of analysis († = Applied with ATP (10µM)). Application of drug (marked as red arrow) occurs at 120s from start of recording. Each example trace represents individual cell ROI identified from image (dashed line indicates 1 F/F_0). **(B)** % of cells per coverslip responding measured as F/F_0 increasing above >3 SD threshold. ATP (10µM) (n=22) shows reliable calcium response in cortical cells that is significantly blocked by PPADS (100µM) (n=5) (**, P=0.0080 vs ATP) and suramin (100µM) (n=4, **** P=<0.0001 vs ATP). ATP induced calcium response fails to be significantly blocked by either $P2Y_1$ or P2X selective antagonists individually, MRS2179 (20µM) (n=6) (ns, P=0.8631 vs ATP), TNP-ATP (1µM) (n=2) (ns, P=>0.9999 vs ATP). **(C)** Fold change Max (F/F_0) of responding cells shown as mean (top) and of each individual cell analysed (bottom). Responding astrocytes show significant changes in fluorescence response in the presence of PPADS and suramin compared to ATP (****, P=<0.0001 vs ATP). However selective antagonist TNP-ATP showed no significant changes in fluorescence response (ns, P=0.9975 vs ATP). MRS2179 significantly decreases the initial calcium response of ATP (****, P=<0.0001 vs ATP).

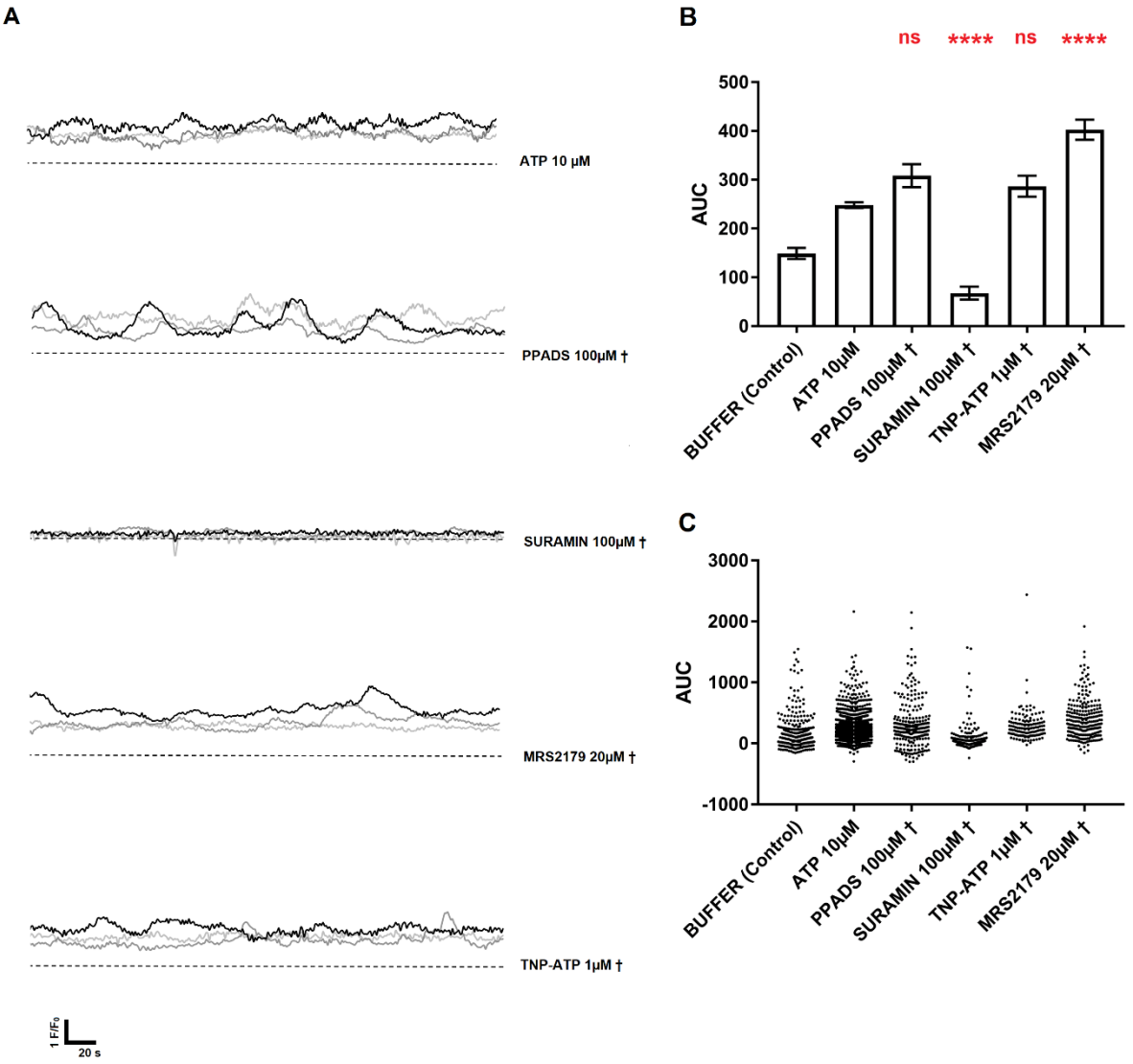

Figure 3.5. Late-Stage Calcium Signalling in Cortical Astrocyte Cell Culture in Response to ATP. (A) Fluorescence traces of single cell ROIs displaying F/F_0 over time during exposure to ATP (10µM), PPADS (100µM) † and suramin (100µM) †, TNP-ATP (1µM) † and MRS2179 (20µM) †, for time period of analysis († = Applied with ATP (10µM)). Time period of analysis for late-stage response, traces show 900s to 1200s. Each example trace represents individual cell ROI identified from image (dashed line indicates 1 F/F_0). Traces are selected as representation of mean data and only shows 3 individual cell responses each. **(B)** AUC ($(F/F_0)/(s)$) with a background normalisation is analysed for 300 frames (900-1200s) to determine calcium signal propagation and regeneration in the cortical astrocytes over a longer period. PPADS (ns, P=>0.9999 vs ATP) and TNP-ATP (ns, P=0.0.0781) both show no significant effect in the late phase calcium response in relation to ATP alone. The only antagonist to significantly reduce the calcium response during this period was suramin (****, P=<0.0001 vs ATP). MRS2179 causes a significant increase in the calcium response in the final 300 s (****, P=<0.0001 vs ATP) **(C)** AUC of each individual cell displays the large variance of the responses observed when totalled from each coverslip, data shown to not to be normally distributed (P=<0.0001). Some cells drop below the baseline response of 0, this represents cells where fluorescence declines below the baseline at the start of the experiment.

3.4 DISCUSSION

The goal of this investigation was to analyse whether ATP release contributed to calcium signal generation and/or propagation within cultured cortical astrocytes. By viewing the astrocyte calcium response over a 20 min period, it was possible to investigate the initial response to an applied stimulus, and later downstream autocrine or paracrine signalling theorised to occur through the release of ATP as a gliotransmitter.

The initial application of glutamate to the cortical astrocytes provided a mimic for presynaptic release of neurotransmitter, heavily supported in literature to initiate increases in intracellular calcium in astrocytes (James & Butt, 2002; Nedergaard, et al. 2003; Lalo, et al. 2008), but would persist in the bath solution providing an experimental setup that allows an equilibrium response to sustained stimulation to be also be measured. The summation of these intracellular events is understood to produce a global calcium signal throughout the astrocyte and continued signal propagation from cell to cell in a wave like response. Therefore, a P2 purinergic antagonist such as PPADS, should reveal any fraction of the calcium signal observed with an initial glutamate stimulus that was due to ATP release (Pangršič, et al. 2007; Parpura & Zorec, 2010).

Our results show that PPADS did not reduce the calcium response to either the initial response, or to later, prolonged periods of stimulation. In fact, there was a significant increase in the mean AUC for cells treated with both glutamate and PPADS (Figure 3.3B). This opposes literature where ATP has been shown to be the main extracellular messenger for calcium wave propagation in cultured astrocytes via receptors sensitive to PPADS, although stimulation was performed mechanically and in an electrical manner (Guthrie, et al. 1999). It is possible that the pattern or train of stimulation used to simulate neuronal transmission is key to the involvement of specific gliotransmitters in signal propagation. In the sustained exposure to glutamate used here, PPADS-sensitive receptors appear to have a small inhibitory effect on persistent calcium signalling.

To test for purinergic signalling mechanisms and receptors involved in inducing calcium signalling in the cortical astrocytes in more detail, the same protocol was applied using ATP as agonist. In these experiments, PPADS significantly reduced but did not eliminate ATP-induced calcium responses in the initial phase (Figure 3.4B). The effectiveness of suramin provided a superior block to the initial calcium response, significantly reducing the percentage of cells responding and the maximum fluorescence change (Figure 3.4B, C) This may provide a useful tool for future use in tissue investigations assuming that receptor isoform expression is similar in situ to in culture.

In late-stage calcium signalling, purinergic signalling is once again shown to be complex in relation to sustained astrocyte calcium signalling. PPADS reduced the initial response to ATP but had no significant effect on late-stage calcium responses. This suggests that some PPADS-sensitive isoforms of purinergic receptors contribute to the initial calcium response but not to later responses.

The response to suramin was closer to predictions for a broad-spectrum antagonist of P2 receptors, causing a significant reduction of calcium signalling during both initial and late periods of stimulation (Figures 3.4B and 3.5B). Suramin has previous displayed success in

similar investigations for cortical astrocyte ATP release and calcium signal propagation (Fumagalli, et al. 2003).

The different responses induced by the two broad-spectrum antagonists in early and late phase calcium responses highlights a complex pharmacological mechanism. This could be due to isotype selectivity differing between the two. PPADS is a widely used broad spectrum inhibitor of the P2 receptor group, its antagonistic effects are especially efficient on the $P2Y_1$ receptor subtype (Jacob, et al. 2014). PPADS has previously been shown to be effective in astrocyte populations blocking ATP induced currents through investigation of P2X subtypes also (Lalo, et al. 2008) – and further disrupts ATP accumulation in the extracellular space, indicating a reduction in ATP (Svobodova, et al. 2018).

More targeted pharmacology showed that neither of the selective antagonists used for blocking P2Y and P2X receptor classes individually had a significant impact on the percentage of cells responding (Figure 3.4B). This indicates that the calcium signal is composed of multiple subtypes of P2Y and possibly P2X receptors, with no obvious subtype (at least sensitive to these inhibitors) dominating the signal. The $P2Y_1$ receptor has previously been shown to be widely associated with increased calcium concentrations intracellularly and activation of the propagating calcium waves (James and Butt, 2002). Specific targeting of this subtype with MRS2179 failed to provide a significant block to cells responding to the ATP but did significantly reduce the max induced calcium concentration increase in our experiments (Figure 3.4C). Blocking of specific $P2Y_1$ related calcium response to ATP highlights the multi-faceted mechanisms for inducing an increase in intracellular calcium concentration, in which cell recruitment is unaffected but the level of response is significantly reduced. This could be supported by the role of metabotropic receptors producing larger calcium responses that propagate the whole cell compared to other P2 receptor subtypes. Here astrocytes possess a broad spectrum of P2 receptor subtypes in its physiology with evidence of expression in rat tissue for $P2Y_1$, $P2Y_2$, $P2Y_4$, $P2Y_6$, $P2X_{1\text{-}5}$ and $P2X_7$ (Fumagalli, et al. 2003).

P2X subtypes are seen in expression study for rat cortical tissue (Fumagalli, et al. 2003), and provide another interesting mechanism for calcium signalling however primarily in a more ionotropic function, where P2X7 receptors can form non-specific cation permeation channels for Ca^{2+} influx and Na^{+} for voltage gated Ca^{2+} channels operation and furthermore an activation dependent pore size (James & Butt, 2002). The expression of these receptors along with P2Y subtypes has shown a supporting function of purinergic activation for increased calcium concentration within the astrocytes (James & Butt, 2002). However, much like that of the MRS2179, specific targeting of the P2X receptor subtypes with TNP-ATP failed to provide a significant blockade of ATP induced calcium response in cultured astrocytes, to a lesser extent than that of the P2Y specific inhibitor. (Figure 3.3B).

Late phase analysis of the astrocyte calcium responses showed varying results to the metabotropic and ionotropic purinergic antagonists. Here TNP-ATP does not result in any significant change to the calcium response in comparison to ATP alone, but MRS2179 did display a significant increase in AUC of calcium response, showing a similar enhanced response to that observed in application of PPADS with glutamate. This would suggest that P2Y receptors may provide a negative feedback effect during prolonged astrocyte calcium signalling. This data proposes a difficult question into the relation of purinergic signalling and its link to astrocyte calcium signal propagation. However, there is some evidence that P2Y

receptors may have a dual control of calcium release of internal stores via IP_3R activation – with a report suggesting that P2Y mediated signalling can provide a negative feedback effect on intracellular calcium concentrations in smooth muscle cells (MacMillan, et al. 2012).

In conclusion, it seems that while multiple isoforms of purinoreceptor can initiate large scale calcium responses in cultured astrocytes, autocrine or paracrine ATP release does not contribute a substantial fraction to the calcium response generated by short-term or long-term exposure to glutamate. There is some evidence that PPADS and MRS2179 sensitive P2Y receptors may in fact reduce late phase regenerative calcium signalling, although variance in the data makes interpreting this result difficult.

Cultured cortical astrocytes were the main in vitro model used to establish the role of extracellular ATP in signal propagation in the literature and allowed for the validation of experimental methods and pharmacology in a well-controlled experiment with a pure population of astrocytes. Despite this, there are obvious limitations for interpreting how in vitro pharmacology relates to in vivo signalling. The next stage of the investigation was an attempt to understand how these results compare to calcium propagation in specialized Bergmann glial cells in situ in acutely isolated cerebellar slices.

4 Cerebellar Tissue Slice Stimulation

4.1 Introduction

The cell bodies of Bergmann glia are adjacent to the neuronal cell bodies in the Purkinje cell layer of the cerebellar cortex, and project fibres through the molecular layer to the pial surface (Hoogland & Kuhn, 2009). Glial microdomains adorn the Bergmann fibres, and compartmentalize the synapses of neurons within the molecular layer. These distinctive structural formations form a basis for signalling between the neurons of both pre- and post-synaptic cells with the surrounding glia –which has become named the 'tripartite synapse' (Perea, et al. 2009). Localised transmembrane proteins are expressed within the microdomains, including uptake transporters and receptors for the extracellularly diffusing neurotransmitters (De Zeeuw, & Hoogland. 2015).

An aspect of Bergmann glia function that affects signalling is the uptake mechanisms that terminate the transients of glutamate in the synaptic cleft through rapid uptake and recycling. The presence of transporters, such as EAAT1, on the Bergmann glia reduces the glutamate in the extracellular space, reacting to the firing of the parallel fibres in the cerebellum (De Zeeuw, and Hoogland. 2015). The high level of expression of EAAT units within the Bergmann glia allows the response to be adapted to extracellular glutamate levels supporting synaptic signalling (Hoogland & Kuhn, 2009). Here glial transporters limit the diffusion of glutamate to nearby synapses regulating signalling specificity and moderates the activation of postsynaptic receptors following prolonged release of glutamate (Bellamy & Ogden, 2005).

Each Bergmann glial cell receives information from, and feedbacks to, many neurons in response to spatiotemporal patterns of synaptic transmission – ultimately aiding in synaptic plasticity of the cerebellum in both inhibitory and excitatory pathways (Bellamy & Ogden, 2005; Bellamy, 2006).

Bergmann glia can respond to different neurotransmitters present within the extracellular space, diffusing from excitatory and inhibitory neuronal elements in the molecular layer. Here glutamatergic (AMPA, mGluR1) and purinergic (P2Y, P2X) receptors expressed on the Bergmann glia, along with $GABA_A$ receptors allow the cells to react to both excitatory and inhibitory transmissions (Brockhaus & Deitmer, 2002; Riquelme, et al. 2002).

These receptors allow Bergmann glia to detect and respond to synaptic transmission, which lead to the induction of intracellular calcium signalling in response to parallel and climbing fibre stimulation (Beierlein & Regehr, 2006). The calcium signalling of the Bergmann glia can be limited to microdomains or propagate to neighbouring glial cells potentially enabling modulatory changes throughout the molecular layer for both neurons and the glia themselves (Hoogland et al, 2009).

An increase in calcium signalling is implicated in morphological changes of the glia, increasing the proximity of the uptake mechanisms in areas that envelop the synapses (Nedergaard, et al. 2003; Lippman Bell, et al. 2010; De Zeeuw & Hoogland, 2015). Furthermore, Bergmann glia calcium waves can have a maintenance and neuroprotective effect, through increased ionic buffering and removal of neurotransmitter from the extracellular space. Downstream, calcium signalling may have consequences in controlling the metabolic activity of neurons through

control of local blood flow (Nedergaard, et al. 2003; Takano, et al. 2005), the conversion of ATP to adenosine (Piet & Jahr, 2007; Araque, et al. 2014), and accumulation of lactate as a neuronal energy source (Caesar, et al. 2008)

4.1.1 Neuron-Astrocyte Signalling

Locally triggered calcium responses seem to act as a self-modulatory mechanism for the synapse, this is uniquely observed in ectopic release of neurotransmitters to the glial sheath (Dobson, et al. 2018). This site is functionally independent from responses at postsynaptic neurons, with distinct calcium channels regulating presynaptic release, and extrasynaptic receptors that are pharmacologically independent and differ temporally from postsynaptic currents (Matsui & Jahr, 2006; Dobson, et al. 2018). This route for communication can exhibit short-term and long-term plasticity that is independent of the adjacent synapse (Bellamy, 2006). At ectopic sites, vesicles are distributed outside of the active zone, for a distinct neuron-glia signalling route. It is hypothesised that this allows for the morphological changes mediated via AMPA receptors to regulate glutamate uptake around the Purkinje neuron synapses, to aid in synaptic efficacy.

Signalling within the cerebellum between glia and neurons is bi-directional. The release of gliotransmitters such as glutamate have been shown to also elicit reductions in neuronal activity within the cerebellum (Brockhaus & Deitmer, 2002). Studies have determined that reductions in spontaneous postsynaptic activity occur as glutamate is released from depolarized Bergmann glia, acting on the presynaptic ionotropic AMPA receptors (Brockhaus & Deitmer, 2002). The release of gliotransmitters has also been shown to not directly lead to the activation of postsynaptic mGluR receptors on the Purkinje neurons, suggesting more of a modulatory role for glial released transmitters (Beierlein & Regehr, 2006).

4.1.2 Parallel fibre signalling to Bergmann glia

Stimulation of parallel fibres can elicit changes in the intracellular calcium of the Bergmann glia, which spread from the site of initiation within the microdomains throughout the glial cell (Beierlein, 2013). In vivo it has been demonstrated that the calcium wave initiation from the source of the glia can span multiple glia in the cerebellum (Hoogland, et al. 2009; Nimmerjahn, et al. 2009).

Bergmann glial calcium signalling has been shown to be biphasic in response to parallel or climbing fibre stimulation, displaying a faster short phase mediated by ionotropic AMPA receptor activation, and a secondary phase mediated by metabotropic activation of both P2Y and mGlu1 receptors and release of cytosolic calcium stores for an initiation of a global signal (Beierlein & Regehr, 2006; Piet & Jahr, 2007).

Unlike other astrocytes, the Bergmann glia express AMPA receptors that lack the GluA2 subunit (Bellamy & Ogden, 2005), increasing calcium permeability and causing influx of calcium ions in a short and localised manner (Nedergaard, et al. 2003; Lalo, et al. 2006). Pharmacological blocking of these components can show observable inhibition of each phase during neuronal stimulation, in which parallel fibre or Purkinje neuron activation have differing components for initiating glial calcium waves (Piet & Jahr, 2007).

The initiation of calcium waves has been reliably reproduced in Bergmann glia (Piet & Jahr, 2007; Hoogland, 2009). Much like that of astrocytic waves, the radially expanding response starts from an initial stimulus. The calcium wave progresses from the connecting microdomain propagating throughout the cell and then into a transglial response. This transglial response requires the local release of gliotransmitters for wave generation as they diffuse three dimensionally between the Bergmann glia in the molecular layer (Hoogland, 2009). This release can also use intermediates such as parallel fibres or interneurons for cell-to-cell signalling, leading to further ATP release (Hoogland, et al. 2009). This mechanism within the cerebellum could aid in the signal propagation within functional domains encompassing purkinje cell spines and interneurons for local plasticity (Araque, et al. 2014).

The glutamate and ATP that initiate the glial calcium signalling have multiple potential origins within the molecular layer. The release of ATP from the parallel fibre synapses, interneurons and from Bergmann glia themselves offer a potential trigger for P2Y activation in the Bergmann glia (Piet & Jahr, 2007). Whereas the release of glutamate is established from parallel fibre activation offering a signalling mechanism for mGluR1 activation on both Purkinje neurons and Bergmann glia (Beierlein & Regehr, 2006). Observations of antagonising both mGluR1 and P2 receptors eliminates the calcium signalling of the Bergmann glia in response to synapse activation, however inhibiting AMPA receptors did not disrupt calcium transients entirely (Beierlein & Regehr, 2006). This displays a key role for metabotropic receptors in signal propagation.

4.1.3 Calcium Signalling at different stimulation frequencies

Preceding work in the laboratory forms the basis of this investigation. Here stimulation of the parallel fibres produces a calcium response that propagates from the adjoining microdomains through the whole cell structure, ultimately reaching the soma of the Bergmann glia (see Introduction, Figure 1.4). The global response is optimally observed following a stimulation train of 10 pulses at 30 Hz.

It has been previously noted that a stimulation protocol of 16 Hz frequency for 15 s causes LTP of the parallel fibre to Purkinje neuron synapse (Hartell, 2002; Dobson & Bellamy, 2015). However, this same 16 Hz tetanus leads to a robust spatial inhibition of Bergmann glial calcium responses evoked by 30 Hz trains. This phenomenon represents long-term depression of glial response propagation under the same conditions that cause long-term potentiation of the synapse. This preliminary result suggests that the spatial propagation of calcium signals in Bergmann glia can be modulated by patterns of activity that cause synaptic plasticity. To understand the computational implications of this observation, we need a better understanding of the mechanisms that regulate calcium wave propagation in Bergmann glia.

To extend the investigation of this phenomenon, we had two aims: to develop a method for bulk loading of Bergmann glial cells in cerebellar slices and to reproduce and investigate the mechanisms responsible. This protocol was used to increase the throughput of experiments (as single cell patch clamp recordings are technically demanding and time consuming). To be successful the protocol developed would produce a way to successfully screen antagonists in situ to investigate the components of the calcium response at different stimulation frequencies using a simpler protocol.

This protocol was used to reproduce the key observations made using single-cell recordings, and then screen the receptor types involved in signal propagation in Bergmann glia, building on the results observed in cultured cells.

Finally, we also tested a candidate mechanism for the long-term depression of Bergmann glial calcium spatial range: serotonin receptors. Synaptic modulation is further involved with messengers such as adrenaline, dopamine, serotonin and nitric oxide capable of mediating transmission for plasticity changes in neuronal elements, such as parallel fibres and Purkinje cells, and astrocytes (Fages, et al. 1994; Peng, et al. 2005; Croft, et al. 2015; Dobson & Bellamy, 2015), but an initial screen suggests these receptors do not contribute to spatial plasticity. The involvement of astrocytes in neuromodulatory pathways could highlight plasticity elements not yet appreciated – particularly with serotonergic receptor densities observed in cerebellar astrocytes (Verge, et al. 1991; Dieudonné, 2001)

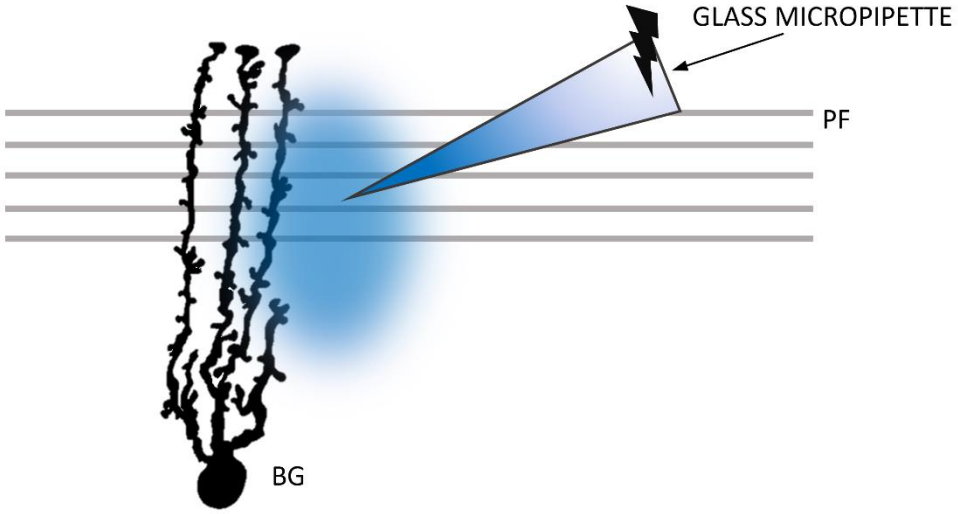

Figure 4.1 Bulk Extracellular Loading and Stimulation Protocol. This protocol is used to investigate the calcium response of Bergmann glia in cerebellar slices following stimulation. Here the glass micropipette is loaded with Fluo5F-AM and positive pressure allows the indicator to diffuse into the molecular layer, as depicted. After loading, direct stimulation of the molecular layer is delivered via the micropipette, stimulating the Parallel Fibres (PF) and eliciting a calcium response in Bergmann Glia (BG). Differing tetanus can be delivered in this protocol to investigate Bergmann glia plasticity and the propagation of calcium response when imaged via microscope in a less technically demanding manner. This proposed protocol will allow for efficient investigation of BG calcium responses independent of single cell patch clamp.

4.2 Methods

Preparations of the cerebellar slices and the final loading and stimulation methodology is described in section 2.5-7. And final refined protocol obtained as stated in investigations in section 4.3.

The preparation of the pharmacology is prepared within Krebs Buffer (supplemented with 2mM $CaCl_2$, 1mM $MgSO_4$) at room temperature unless stated otherwise. Drug was applied via bath perfusion. In instances of buffer control, Krebs Buffer is continued perfusion at a similar rate to that of drug infusion.

PPADS (100 µM) and suramin (100 µM) were prepared as before within section 3.2, to maintain comparability between cell culture and slice preparations. NBQX was prepared in distilled water vehicle for dilution to a final concentration of 10 µM. CPCCOEt was prepared within DMSO with final concentration of 100 µM in 0.5% DMSO when delivered. Asenapine is prepared within DMSO but with final concentration of 100 nM in 0.001% DMSO after dilution into Krebs Buffer.

Parallel fibres were stimulated with a glass electrode positioned within the molecular layer that was also used to apply Fluo5F-AM to the slice (Figure 4.1). Stimulation was carried out with a constant-current isolated stimulator at 100 µA (80 µs).

One-way ANOVA is used to compare the AUC (ΔF/s) change (ΔF Ratio) between calcium responses in the presence and absence of antagonist: a value of 1.0 would indicate no change in ΔF. ΔF indicates the change in fluorescence relative to background fluorescence. Asenapine data compared to that of Buffer in 16 Hz knockdown of 30 Hz investigation as an AUC change (ΔF Ratio) also. ΔF Ratio represents the difference between pre- and post-16 Hz stimulation response, a value of 1.0 would indicate identical response (AUC) Data here is compared using an unpaired t-test with Welch's correction. This test is selected to compare the two unpaired data sets with unequal variance and equal sample size.

4.3 Results

4.3.1 Protocol Refinement

Bulk loading of fluorescent calcium indicator into the molecular layer of cerebellar slices was carried out to test for extracellular uptake by glia and labelling of Bergmann fibres as distinct structures within the field of view. Positive pressure was applied to a glass microelectrode (~ 1 MΩ resistance) containing Fluo5F-AM positioned within the molecular layer, to allow for expansive loading of the tissue slice. The rationale for this approach is that Bergmann fibres should be discernible as lateral processes that run through the molecular layer perpendicular to the Purkinje cell layer (Figure 4.2).

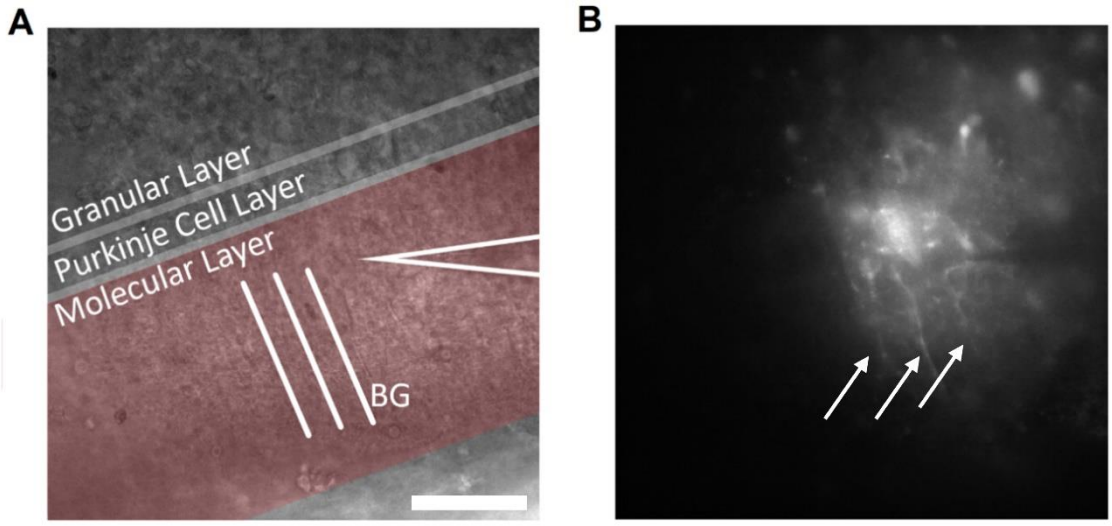

Figure 4.2. Extracellular Loading of Calcium Indicator in Cerebellar Slice (A) Outlines of the observable layers in the transverse slice of cerebellum with brightfield microscope identifies location for placing of micropipette loaded with Fluo-5F (100µM**)** (Scale bar = 50 µm) **(B)** Indicator viewed through wavelength filter and excited at 480nm shows loading of Bergmann glia (BG) fibre-like structures (arrows).

4.3.2 Bergmann glial cell Loading

n initial investigation of the extracellular tissue loading, the loading of the Fluo-5F AM was performed using modest positive pressure (applied manually) of the glass micropipette positioned in the molecular layer of the slice and applied into the slice for 30 minutes. Different concentrations of the fluorescence label were tested (10µM, 20µM, 100µM). Imaging of the tissue slices at 10µM or 20 µM Fluo-5F AM can result in a visible loading of the Bergmann glia and surrounding structures of the molecular layer, but labelling was weak at times and results were inconsistent. The maximum concentration tested was 100µM, which more consistently produced a clear loading of tissue and strong uptake of labelled calcium into the cells present in the molecular layer (Figure 4.2B). 30 min application of 100 µM Fluo5F-AM was therefore adopted as the standard protocol for bulk loading.

4.3.3 Stimulation

Stimulation of the slice post-loading was applied via the same micropipette, to eliminate any further damage to the tissue and isolate the stimulation to the region of fluorescent loading.

Stimulation of the slice was initially delivered at 10 pulses at 30Hz as this produced a large increase in local fluorescence measured within the region of interest (ROI). Stimulation of the molecular layer with this protocol provokes an optimal glial calcium response in single cells (Introduction, Figure 3), and results in an intense increase in fluorescence at the point of stimulation in bulk-loaded slices, that is followed by propagating calcium waves that spread perpendicularly to the direction of the parallel fibres (Figure 4.3A)

Stimulation of the molecular layer with a different protocol designed to evoke long-term plasticity (16 Hz, 15 s) results in a widespread increase in fluorescence intensity throughout the stimulated region of the slice. Although the perpendicular propagation along structures resembling Bergmann fibres can still be observed by eye, it is overwhelmed by signals which will originate from any cellular element (neuronal or glial) that accumulated Fluo5F (Figure 4.3).

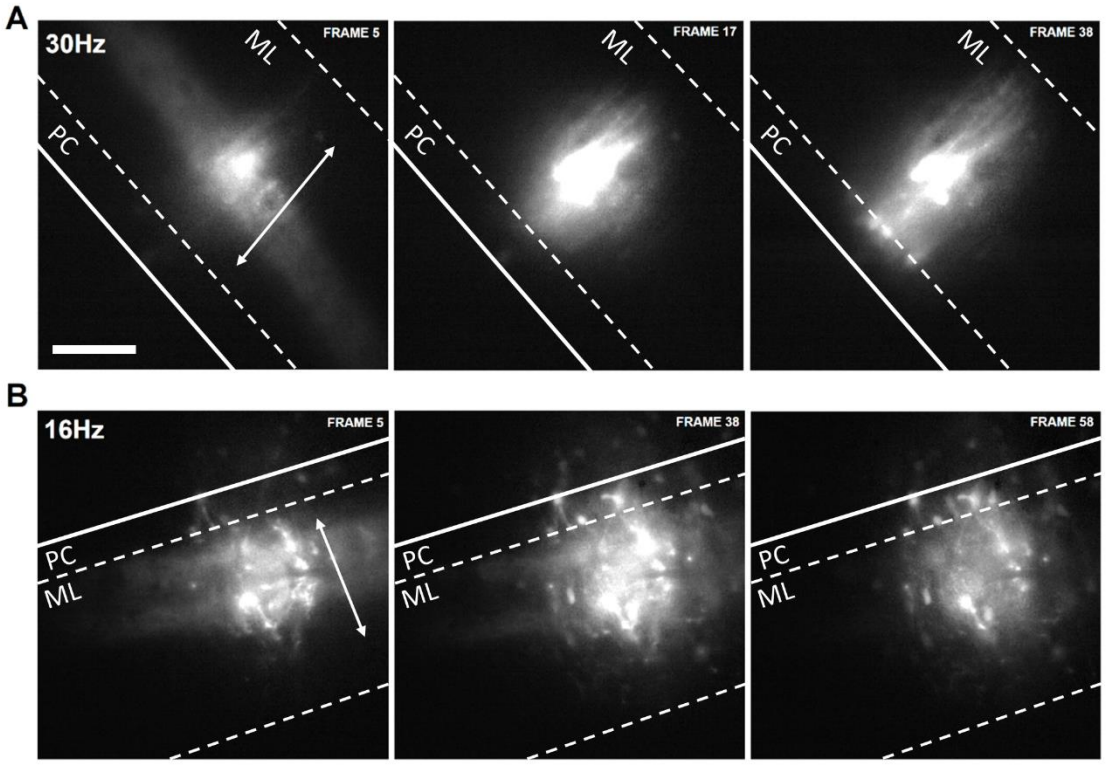

Figure 4.3. Stimulation Landmarks in Slice Stimulation. Following stimulation, observable landmarks can be highlighted that differ between frequencies in these examples slice imaging stacks (1 Frame = 0.3 s). Dashed line denotes the molecular layer (ML) and solid line to dashed indicating the Purkinje cell layer (PC), with the arrow indicating loaded Bergmann glia fibres and the indicated alignment (Scale bar = 50 µm) **(A)** At 30 Hz stimulation, parallel fibre signal is observed at initiated time of stimulation, seen as hazy lines spanning in line with the fibre bundle (Frame 5). Parallel Fibre response is present for only a single frame due to the short duration of stimulation (10 pulses). Glia response is clearly pronounced and spreads perpendicular to parallel fibre in wave like movement (Frames 17, 38). Response in Frame 38 shows the Bergmann glia response reaching the PC layer **(B)** 16Hz stimulation of the slice shows parallel fibre firing at the instance of stimulation (Frame 38) glia response is seen overlapping perpendicular to that of the parallel fibre signal as an observable wave (Frame 58), which continues after stimulation of the slice stops and parallel fibres are no longer observed.

4.3.4 Analysis Refinement

Refinement of analysing the raw data required a tailored analysis to partially isolate the glial signal in a busy image consisting of overlapping components. Raw data images are processed within ImageJ. Multiple strategies were tested, the high noise images were isolated of background loading by removing an average of the first 3 frame of the stack and then subtracted from the whole stack, producing image stacks seen in Figure 4.3. This allows pre-stimulation background to be removed and only the pixels that change due to stimulation to be analysed – resulting in images measured for ΔF.

The glial signal is isolated partly by masking overlapping parallel fibre firing which is noticeable as a band running through the centre of the image. The positioning of an oval shaped ROI that is identified by eye removes the majority of the parallel fibre signal and selects for fluorescence changes that propagate laterally away from the central region associated with the fibre volley.

Using this analysis method, changes in mean fluorescence intensity within the ROI were plotted and revealed multicomponent responses (Figure 4.4). Traces displayed for both 30 Hz and 16 Hz stimulation show a fast acting and slower acting component (Figure 4.3). These components of the trace and the raw images can help display activation of calcium signalling of cellular components in the molecular layer. Although we have to accept the limitation of a mixed neuronal and glial signal, it is also possible to relate the kinetics of the response to existing literature.

The fast acting intial spike can not be definitively described as a neuronal component, however it aligns with similar kinetics and a joint secondary glial response also seen (Beierlein & Regehr, 2006; Brenowitz & Regehr, 2014). In a similar protocol Benowitz & Regehr, 2014 looked at the fluorescene calcium response of parallel fibres, showing the response of them is rapid with small onset, decaying over time. Paired with data obtained from Bergmann glia specific stimulation (Beierlein & Regehr, 2006), response traces showed an onset at around the 1 s mark and peak at 1.7 s with a more rounded decay. The data observed in 30 Hz traces shows distinguishable that fast responding neuronal response, followed by a slow decaying glia response (Figure 4.4). Similarly, the kinetics of the perpendicular spread of calcium closely matched the time course and spatial pattern of individually-loaded Bergmann glia recorded under the same experimental conditions (Introduction, Figure 1.3). Therefore, although we cannot definitively rule out a neuronal component to this signal, we can conclude that it closely resembles Bergmann glial responses as measured by us and others.

We also quantified calcium responses as the AUC of the mean change in fluorescence after stimulation had ceased to further isolate the glia contributions to the imaged fluorescence response.

For 16 Hz stimulation, the signal is much more complex. During the prolonged 15 s stimulation window, multiple sources of increased fluorescence intensity are evident. This results in a broad increase in mean signal in the ROI that precludes isolation of individual kinetic components (Figure 4.4B).

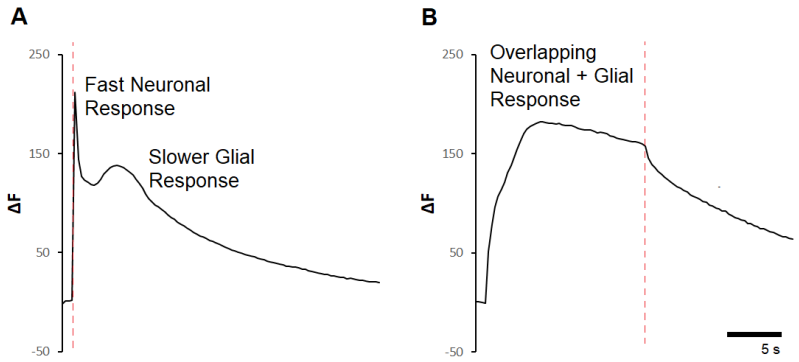

Figure 4.4. Calcium Fluorescence traces of 16 Hz and 30 Hz stimulation. Example traces of both stimulation frequencies, with stimulation beginning at t=1s and the red line displaying the end of stimulation. (**A**) 30 Hz stimulation is brief and shows Parallel Fibre and Glia responses that are identifiable in the trace – neuronal response is fast with the onset of Glia calcium response later and slower. (**B**) 16 Hz stimulation given over a prolonged period shows overlapping neuronal and glial components that are not individually distinguishable. Parallel fibre firing seen in Raw Data overlaps Bergmann Glia response during stimulation.

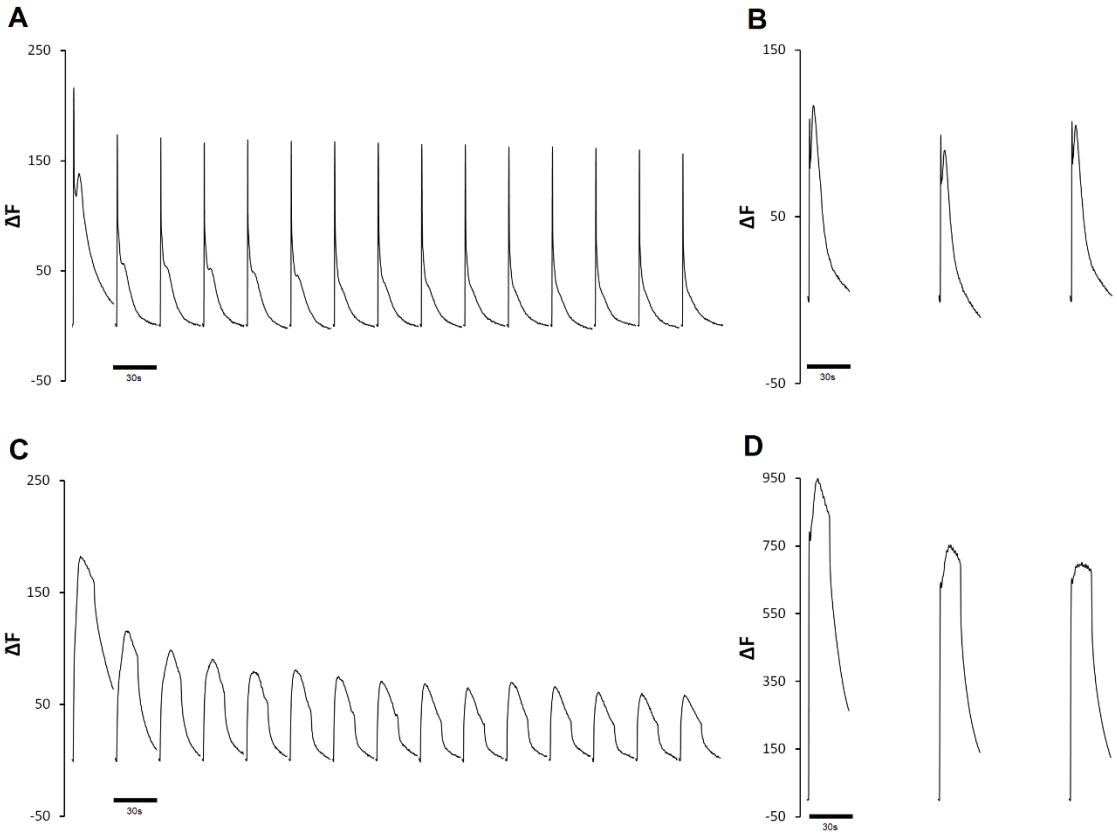

Figure 4.5. Repetitive stimulation of parallel fibres at different frequencies. Repetitive stimulation trains for 30 Hz and 16 Hz show a decrease in calcium signal observed with smaller instances of recovery. The timescale of stimulation repetitions for each graph is a total of stimulations within a 30-minute period, key for 30 seconds displays the time imaging of the slice for stimulation. **(A)** 2-minute intervals of 30 Hz stimulation show decrease in overall calcium associated fluorescence (note, line break is start of 1.5 min break before next stimulus). The secondary peak of the each of the stimulation plots with initial peak corresponding with parallel fibre stimulation. **(B)** Intervals with 10-minute recovery between trains shows maintenance of glia corresponding response. **(C)** 2-minute intervals of 16 Hz for 15s stimulations show a decrease in overall response amplitude. **(D)** 10-minute intervals here show overall recovery of calcium response observed.

4.3.5 Stimulation Intervals

Tetanic stimulation was repeated at 2 min intervals to assess the stability of calcium responses but led to a significant decline in calcium response (Figure 4.5A, C). Intervals of 10-minute recovery between repetitions of stimulation produced robust and stable fluorescence responses in response to both 30 Hz and 16 Hz stimulation (Figure 4.5B, D)

This protocol allows for a more reliable test of pharmacological effects and 16Hz-evoked plasticity without concerns about fatigue or run down.

4.3.6 Temperature

Finally, we also tested the effect of temperature on calcium responses. The previous experimentation within cell culture and slices was performed in room temperature solution, but higher temperatures would be more physiologically relevant.

An inline heater was used to raise bath temperature into the 32-37°C range. However, bulk loading was unreliable and inconsistent at this temperature, frustrating attempts to investigate the impact of temperature on calcium wave propagation. Multiple attempts retrieved images that could not be analysed and lacked detail from Fluo-5F AM absorption. Stimulation of the slices as to protocol with poorly absorbed indicator showed faint response that deteriorated in detail over time. This was also observed in a similar protocol by Brenowitz & Regehr, 2014, in which retention of acetoxymethyl indicators was affected at physiological temperatures while bulk loading parallel fibres.

Although this is a limitation that should be addressed in future, we continued with room temperature recordings for the remainder of the project.

4.3.7 Pharmacological analysis of calcium responses

Cell culture data showed that PPADS and suramin produced significant inhibition of astrocyte calcium signals in response to ATP exposure. We therefore tested these compounds on 30 Hz and 16 Hz stimulation in slices.

4.3.8 30 Hz Stimulation

Following 10 min perfusion of 100 µM PPADS onto tissue the calcium signal induced by a 30Hz train was significantly inhibited (Figure 4.6) (***, P=0.0007 vs Buffer). PPADS decreased mean response AUC to 0.497-fold of pre-treatment value.

Similar treatment with suramin produced no significant effect on the calcium response to 30 Hz stimuli (ns, P=0.5464 vs Buffer). This is in striking contrast to the results observed in cultured astrocytes (Section 3.3).

Building upon the inhibition effects of PPADS, previous work has established the parallel fibre induced calcium signalling of glia is a multifaceted mechanism involving both glutamate and purinoreceptors (Section 4.1.2). A combination of AMPA receptor antagonist, NBQX, a

selective $mGlu_1$ antagonist, CPCCOEt, and the broad spectrum P2 receptor antagonist, PPADS, offers an extensive blocking of the bulk-loaded calcium response. (***, P=0.0001 vs Buffer) (Figure 4.6B).

These results demonstrate that the secondary calcium response initiated by a 30 Hz train is consistent with previous reports on the role of both ATP and glutamate release from neuronal components in calcium response in glia (Piet & Jahr, 2006; Beierlein & Regehr 2006) – further supporting the idea that we can meaningfully detect glial signals with this bulk loading protocol.

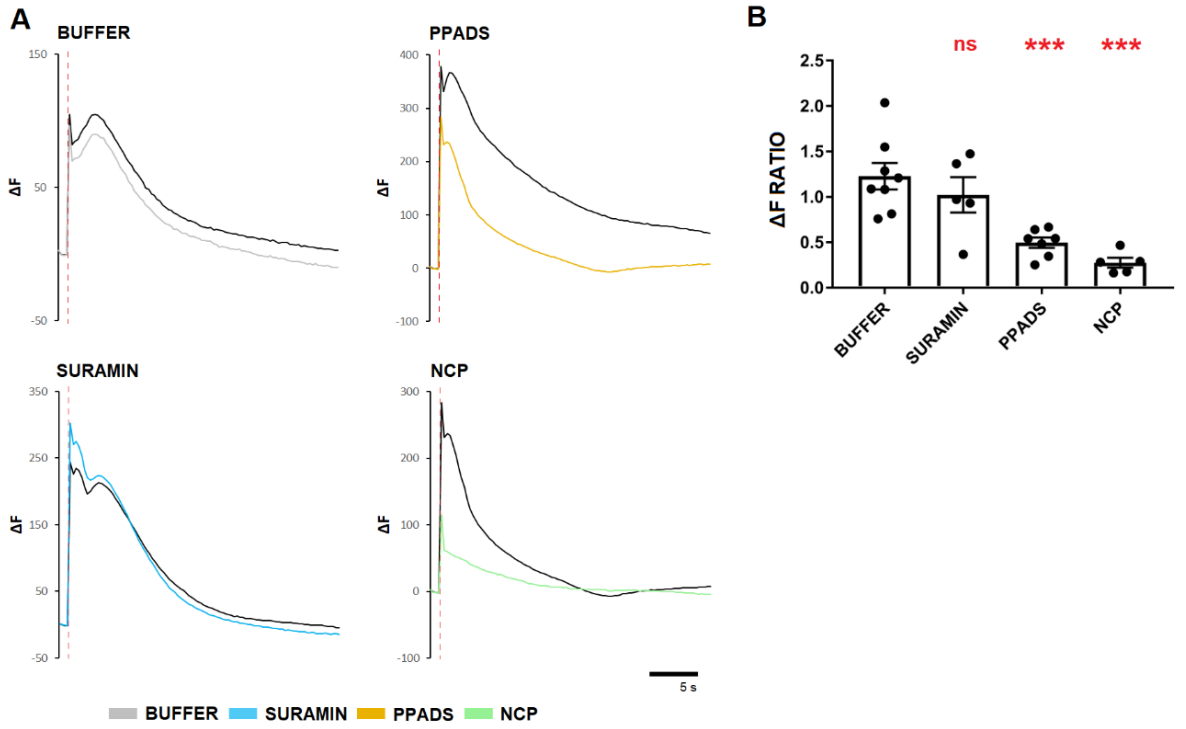

Figure 4.6. Pharmacological analysis of 30 Hz Stimulation calcium response (A) Example traces of 30s post-stimulation of cerebellar slice at 30 Hz. Black traces show 30 Hz stimulation performed in buffer and coloured traces show stimulation performed following 10 min treatment with pharmacology in the same slice. Analysis for AUC performed following the end of stimulation signified by red dashed line. ΔF indicates change in fluorescence in comparison to background. **(B)** ΔF Ratio shows mean ± SEM of AUC before and after addition of antagonist or buffer control. Buffer (n=8 slices) shows stable calcium fluorescence response to 30 Hz stimulation. Addition of 100 µM suramin had no significant effect (n=5, ns, P=0.5464 vs Buffer), but 100 µM PPADS (n=7, ***, P=0.0007 vs Buffer) and a combination of 10 µM NBQX, 100 µM CPCCOEt and 100 µM PPADS ("NCP", n=5, ***, P=0.0001 vs Buffer) showed significant inhibition of calcium response in Bergmann glia to 30 Hz stimulation.

4.3.9 16 Hz Stimulation

The same experiments were carried out for slices stimulated at 16 Hz for 15 s (Figure 4.7A). Here we attempted to isolate glial responses within the decay phase of the fluorescence signal after stimulation had ceased (dashed line in figure), as the response during ongoing stimulus was bound to be significantly contaminated by non-glial components.

Under these constraints, only the combination of antagonists (NCP) significantly reduced calcium response as a result of 16Hz stimulation (*, P=0.0154 vs Buffer).

This experiment confirms the difficulty of effectively measuring glial signals during the LTP-inducing stimulus train.

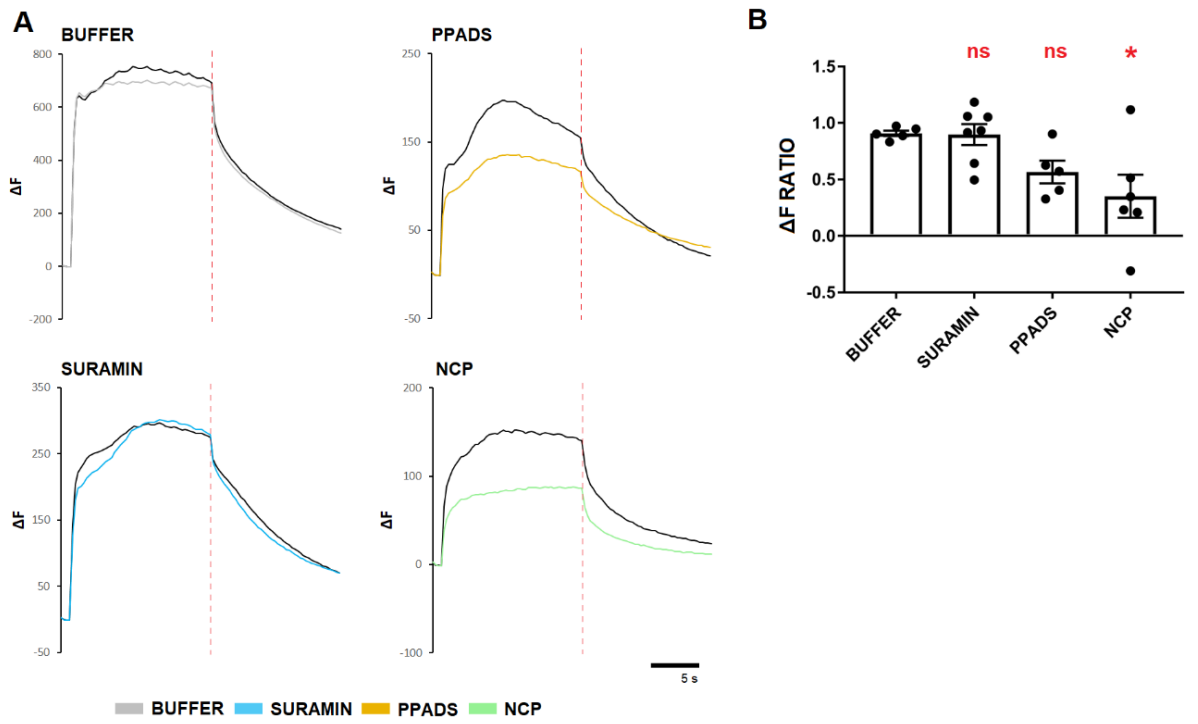

Figure 4.7. Pharmacological analysis of 16 Hz Stimulation calcium response (A) Example traces of 30s post-stimulation of cerebellar slice at 16 Hz. Black traces show 16 Hz stimulation performed in buffer and coloured traces show stimulation performed following 10 min treatment with pharmacology in the same slice. Analysis for AUC performed following the end of stimulation signified by red dashed line. ΔF indicates change in fluorescence in comparison to background. **(B)** ΔF Ratio shows mean ± SEM of AUC before and after addition of antagonist or buffer control. Buffer (n=5) shows stable calcium fluorescence response to 30 Hz stimulation, suramin shows no significant inhibition (n=7, ns, P=>0.9999 vs Buffer) or PPADS (n=5, ns, P=0.1957 vs Buffer) – however PPADS inhibition markedly more. A combination of 10 μM NBQX, 100 μM CPCCOEt and 100 μM PPADS (“NCP”, n=6, *, P=0.0154 vs Buffer) shows significant inhibition of calcium response in Bergmann glia to 16 Hz stimulation.

4.3.10 LTD of glial calcium response Following 16 Hz Stimulation

Previous work using patch clamp recordings showed that the 16 Hz, 15 s stimulus significantly reduced the spatial range of subsequent calcium responses evoked by 30 Hz tetanus. We were able to reproduce this result with the bulk loading protocol (Figure 4.8).

After establishing a clear response to 30 Hz stimulation, a 16 Hz, 15 s plasticity protocol was applied to the slice. Following a 10 min recovery period, a subsequent 30 Hz train resulted in a significantly decreased calcium response, both in terms of the spatial range (Figure 4.8A) and the mean fluorescence change in the ROI (Figure 4.8B). The mean ratio comparing the pre-16 Hz and post-16 Hz 30 Hz calcium signal was 0.328 – reliably showing the reduction in calcium propagation away from the centre of stimulation.

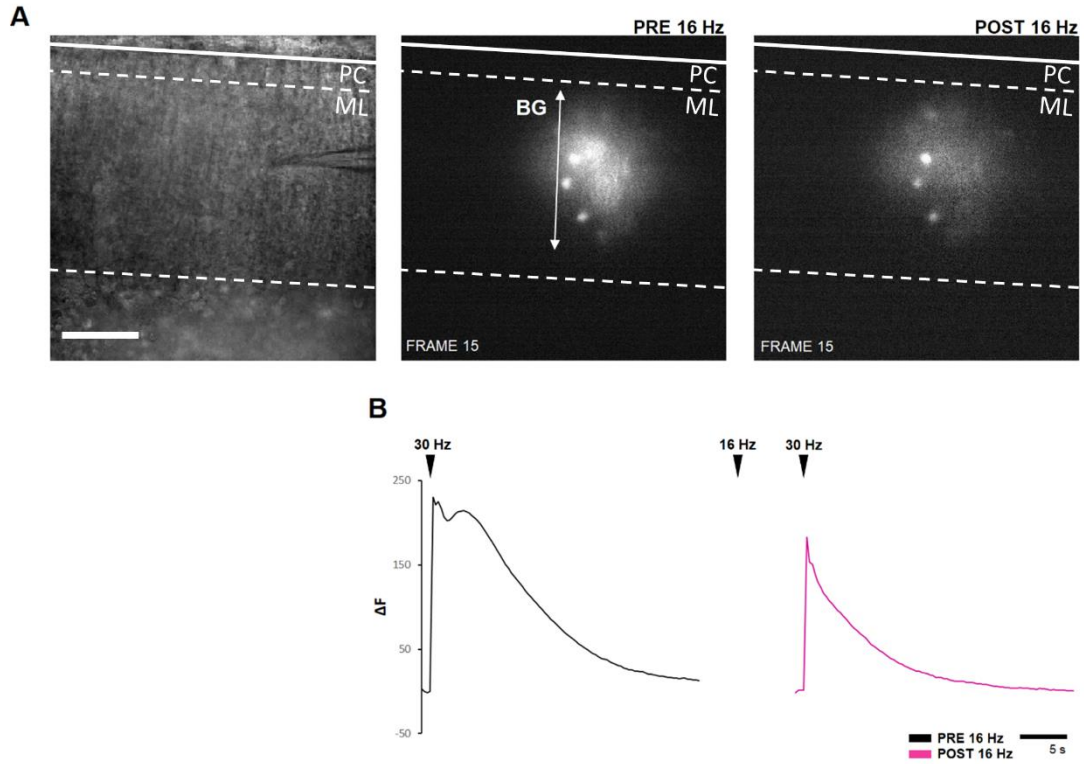

Figure 4.8. 16 Hz initiated Spatial Plasticity of Bergmann Glia Calcium Response (A) Fluorescence loading of acutely isolated cerebellar slices within the molecular layer (ML) (Indicated by dashed area). Microscopy image (left) shows slice orientation and identifiable ML and Purkinje cell layers (PC) (solid line) (Scale bar = 50 µm). Following a loading period, a 30 Hz stimulation of the slice for a produces a control response (Pre 16 Hz) (centre), Image is processed to remove background noise (*see Section 2.7*). Imaging shows a fluorescence wave propagate through the ML towards the PC with fibre like Bergmann glia (BG) (Image taken at Frame 15 to correspond with glial response time max). After a 2 min period a 16 Hz 15s tetanus is applied to induce the spatial plasticity seen previously. Following a 10-minute recovery from this, a 30 Hz tetanus is applied and imaged (Post 16 Hz) (right), this shows a marked reduction in fluorescence response in the ROI and less identifiable Bergmann glia structures. **(B)** ΔF traces for the corresponding stimulus train protocol. Pre 16 Hz (black) trace shows the recognised fast acting neuronal spike and slower onset glial response overlapping in decay (~4.5 s / frame 15). Post 16 Hz (pink) shows an overall reduction in ΔF but shows a clear decrease in the secondary (glial) fluorescence peak corresponding with a reduction in BG calcium response following a 16 Hz 15s stimulus. (Data forms part of analysis, performed under buffer in Figure 10).

A possible candidate for this plasticity mechanism is the serotonergic pathway, that is active within the cerebellum and dense receptor populations in astroglia (Strahlendorf & Hubbard, 1983; Verge, et al. 1991; Takei, 2005). Blocking of serotonin receptors with a non-specific antagonist, asenapine (Frånberg, et al. 2008; Delcourte, et al. 2017), was used to test this hypothesis.

Incubation with asenapine for 10 min before stimulation resulted in an increase in the mean AUC ratio after 16 Hz 15s depression of calcium responses, but this was not statistically significant (ns, P=0.2910) (Figure 4.9A, B).

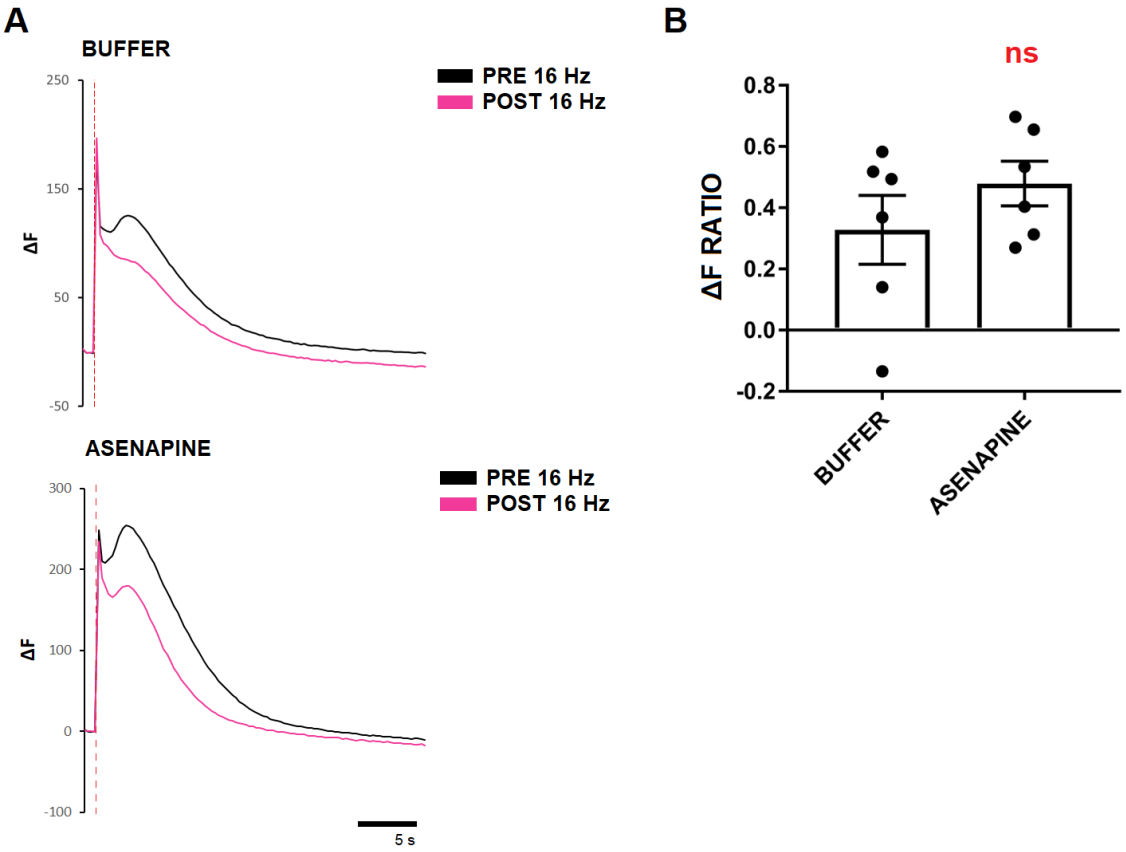

Figure 4.9. Effect of serotonin receptor antagonist on 16 Hz depression. (A) Example traces of 30s post-stimulation of cerebellar slice at 30 Hz. Black traces show 30 Hz stimulation performed in pre-16 Hz and coloured traces show stimulation performed post-16 Hz during treatment of pharmacology. Analysis for AUC performed following the end of stimulation signified by red dashed line. ΔF indicates change in fluorescence in comparison to background 10 min treatment. **(B)** ΔF Ratio shows antagonist effect of pharmacology in comparison of control for buffer with SEM error bars displayed. ΔF Ratio is displayed in the difference in change of AUC fluorescence – here a value of 1.0 would indicate that the response is identical pre- and post-16 Hz stimulation. Buffer (n=6) shows 16 Hz causes a knockdown of following 30 Hz glial calcium fluorescence response. Asenapine 100 nM (n=6, P=0.2910) shows no significant reversal of this inhibition but does show a decrease in 16Hz inhibition.

4.4 Discussion

The objective for this section of the project was to develop a bulk-loading method for measuring calcium signals in Bergmann glia and test the hypothesis that serotonin receptors may contribute to depression caused by 16 Hz stimulation protocol.

The bulk-loading protocol was successful for reproducibly recording fluorescence changes in the molecular layer of acutely isolated cerebellar slices. By refining the protocol and analysis methods, it was possible to largely separate putative parallel fibre and Bergmann fibre responses based on the orientation of the response within the slice and the time course of the responses. However, it cannot be definitively said the glial response is not contaminated with neuronal calcium responses. This protocol does however provide a good foundation for screening pharmacological agents for an effect on the glia calcium responses. Here we were able to demonstrate the signalling responses and previously discovered spatial plasticity can be reproduced in differing protocols.

Pharmacological inhibition of AMPA receptors, $mGlu_1$ receptors and P2 receptors dramatically reduced the calcium responses to 30 Hz stimulation – consistent with previous pharmacological characterisation of Bergmann glial responses (Piet & Jahr, 2007, Araque, et al. 2014). From the plasticity observed, post-stimulus calcium response is dominated by the glial component and aligns with previous literature and expression of receptors successfully blocked (Schipke, et al. 2008). It has previously been shown that the initiation of whole cell signalling occurs through signal summation and multiple receptor stimulation – also leading into transglial signal propagation (Hoogland, et al. 2009; Araque, et al. 2014).

In contrast to our cell culture experiments, PPADS was effective at blocking calcium responses in slices, but suramin was ineffective. This suggests that different isoforms of P2 receptor are present in cerebellar Bergmann glia than cortical astrocytes. Evidence for isoform selectivity has highlighted large overlap between suramin and PPADS, with both having isoform selectivity differences spanning P2Y and P2X subtypes (Syed & Kennedy, 2011). This result is therefore surprising, as it shows a marked difference between cortical astrocytes and the Bergmann Glia, with almost opposite outcomes in sensitivity to the two broad spectrum drugs. Therefore, it cannot be assumed that data can be translated between both cortical astrocytes and Bergmann glia, emphasizing the heterogeneity of the astroglia family. Further differences in preparation spanning cell culture and tissue could also be responsible for this outcome with the presence or absence of other cell types within each study – possibly contributing to how each astrocyte type responds and signals. The presence of neuronal and interneuronal elements within slices is not to be overlooked in the calcium signalling mechanisms investigated, providing further complications in comparing primary culture work to in situ.

The mechanism of 16 Hz stimulation to induce spatial plasticity changes is unknown. Previous experiments within the laboratory have ruled out most of the known modulatory receptor classes at the parallel fibre synapse (unpublished work). Here, the serotonergic signalling was tested as a possible candidate. Serotonergic pathways are involved in surrounding parallel and climbing fibres could induce an encoded signal that localises glia response to specific functional units, seen as spatial plasticity (Araque, et al. 2014). This would provide a threshold for glial response propagation and the modulatory changes initiated by calcium responses in glia would be isolated to a compartment of cellular elements including synapses, interneurons and vascular units.

The basis for serotonergic investigation stems from the neuromodulatory functions of serotonin (5-HT) that have been noted within the cerebellum (Kawashima, 2018). Furthermore, with expression evidence suggesting 5-HT_{1A} and 5-HT_{2A} in astrocytes (Hirst, et al. 1998), it is feasible that this modulatory pathway could contribute to the observed long-term depression. Asenapine, a drug displaying antagonist activity at a large number of serotonin receptor subtypes (along with possible dopamine and noradrenaline inhibition), provided interesting data that offers an insight into the 16 Hz induced mechanisms. The effect of asenapine on 30 Hz stimulation post 16 Hz appeared to show a reduction in the extent of depression of astroglial calcium response in some slices. However, while mean depression appeared reduced, this was not statistically significant. This equivocal result suggests that more data would need to be obtained in serotonin specific receptors and expression to make a satisfactory conclusion.

Overall, we have successfully developed a bulk loading protocol that allows for glial response to be identified within the mixed signal of the molecular layer. This protocol however was insufficient to isolate the detail of Bergmann glia calcium responses for analysis but does offer useful pharmacological screening tool to rapidly advance investigation of glia spatial plasticity.

The mechanism of spatial plasticity in Bergmann glia remains unexplained. One possibility that has not so far been explored is a reduction of ATP release in the molecular layer following 16 Hz stimulation, although the origins of ATP are also unclear. These methods used here have strengths and weaknesses, this investigation has highlighted gaps in the protocol that could be improved. The use of transgenic animals would improve the certainty of glia involvement in the fluorescence response, this would allow for clean definitive results. The use of genetic calcium indicators (GECIs) also could allow for physiological temperatures previously limited due to indicator loading. This will be explored further in the final chapter.

5 Discussion

The main objective of this research project was to understand the factors that control the spatial propagation of calcium waves in astroglial cells. We used cultured astrocytes to investigate how the release of ATP from the cells might contribute to the regeneration and propagation of glutamate-evoked calcium responses. This was investigated both in the early phase of stimulation, and in the late phase of continuous stimulation when cells had been exposed to glutamate for 13-18 min. We also used selective pharmacology to identify the purinoceptors that are expressed by the cultured cells to identify useful tools for intervening in any autocrine/paracrine signalling. This was performed by replicating the investigation of glutamate stimulation with ATP, using broad spectrum and selective antagonists.

Second, we investigated a spatial propagation in acutely isolated slices of rat cerebellum. After developing a protocol for bulk loading acute slices with calcium indicators, we investigated how calcium waves spread through Bergmann glia after stimulation of parallel fibre inputs. Stimulation frequencies were performed to elicit a robust calcium response with 10 pulses at 30 Hz and performed before and after induction of plasticity with a 16 Hz 15 s stimulation protocol. Preliminary results had shown that these calcium waves were dependent on both glutamate and ATP release, and that the 16 Hz plasticity protocol reduced the spatial range of the calcium response in Bergmann glia. Finally, we tested the hypothesis that serotonin receptors may contribute to this spatial plasticity.

The key findings were that ATP release did not contribute to either early or late phases of glutamate responses in cultured astrocytes – in fact, pharmacological evidence suggested that ATP release may inhibit calcium signalling during long-term stimulation with glutamate. We successfully developed a method for monitoring calcium waves in Bergmann glia without the need for patch-clamp recording and showed a significant glutamatergic and purinergic overlap in inducing calcium responses at both frequencies. We were also able to confirm the observation that a 16 Hz protocol reduced Bergmann glial responses, but found that a serotonin receptor antagonist, asenapine, did not significantly alter this plasticity.

5.1 The role of extracellular ATP in astroglial calcium waves

The diffusion of ATP contributes an extracellular transmission path to the spread of intracellular calcium waves in astrocytes. Neuronal stimulation of glia via this pathway has also been shown to be key in initiating a calcium response in astroglia in vivo. The ability for astroglia and neurons to effectively communicate is a strong representation of bi-directional signalling (Perea & Araque, 2005), acting through P2 receptors to initiate downstream mechanisms to increase intracellular calcium concentrations in astrocytes (James & Butt, 2002; Nedergaard, et al. 2003).

Signal propagation is also achieved via diffusion through gap junctions and mobilisation of internal stores, which can also allow the response to be transglial and heterosynaptic in range (Hoogland, 2009; Araque, et al. 2014). This astroglial gap junction signalling has been implicated in synaptic plasticity effects, indicating its relevance for regulating activity in the neuronal network (Chever, et al. 2014). Modulated expression of connexin structures as hemichannels also allow for movement of ATP for inter astrocyte signalling (Chever, et al.

2014; Croft, et al. 2015). The global spread of calcium through astroglial networks can therefore propagate initiating plasticity changes at multiple synapses (Nedergaard, et al. 2013; Araque, et al. 2014).

Glial calcium increases led to activation of exocytosis of ATP (Pangršič, et al. 2007; Harada, et al. 2016; Verderio, et al. 2012). Astrocytes possess the necessary machinery to elicit exocytotic release of gliotransmitters. Complexes such as the N-ethyl maleimide sensitive fusion protein attachment protein receptor (SNARE), vesicle associated membrane protein 2 (VAMP 2) and synaptosome associated protein (SNAP 23) are present within astrocytes and when inhibited, lead to reductions in calcium dependent release of gliotransmitters (Parpura & Zorec, 2010; Verderio, et al. 2012). The release of ATP or glutamate as a gliotransmitter is also reliably blocked with pharmacology effecting intracellular Ca^{2+} buffering and SNARE related mechanisms (Parpura & Zorec, 2010.

We hypothesised that extracellular ATP release from astroglia reported in cultured cells could also contribute to the spread of calcium signals we observe in Bergmann glia in intact slices. Initially, we tested for a contribution of ATP release and P2 receptor activation in cultured primary astrocytes stimulated with glutamate. Our goal was to determine whether the mechanisms of ATP release described by previous reports were relevant to the reinforcement of calcium responses induced by glutamate. Our results showed, in fact, that the broad spectrum P2 receptor antagonist PPADS increased late-stage glutamate responses, contradicting this hypothesis (Figure 3.3). Direct attempts to identify the P2 receptors expressed in astrocytes showed that PPADS was able to partially inhibit the immediate response to ATP but had no significant effect during prolonged stimulation. In contrast, the alternative broad-spectrum antagonist suramin blocked both early and late responses.

P2X and P2Y selective antagonists (TNP-ATP and MRS2179, respectively) applied individually had no effect on immediate responses, but MRS2179 increased calcium signalling during prolonged exposure to ATP, in a similar manner to PPADS in astrocytes stimulated with glutamate. Collectively, these results suggest that the astrocytes express both P2X and P2Y receptors but that suramin is the only effect blocker for the key isoforms contributing to purinergic responses.

In terms of the apparent enhancement of late stage signalling by P2Y blockers, MacMillan, et al. 2012, showed that purinoreceptor, $P2Y_1$, had a dual control over the release of internal calcium stores from the sarcoplasmic reticulum of smooth muscle cell. Here it was found ATP inhibited the IP_3R release of calcium within the cell through a G-protein dependent mechanism that was independent of PLC (MacMillan, et al. 2012). This inhibition was also reversed by MRS2179, a P2Y selective antagonist, confirming the data we have for astroglia calcium response to ATP. This would seem to suggest that with the right combination of pharmacology a similar mechanism can be observed in our primary astrocytes.

Purinergic triggering of calcium waves in glia has been investigated across multiple preparations, with recent developments analysing intact brain in vivo. Specifically, the possibility of the ATP release for astrocyte-astrocyte signalling has been confirmed for glial calcium wave propagation in the cerebellum (Hoogland, et al. 2009; Nimmerjahn, et al. 2009). These calcium waves rely on extracellular ATP contributions for glial signalling, whether this be from the presynaptic terminal, other astroglia or interneurons (Hoogland, et al. 2009; Piet & Jahr, 2007). Transglial calcium responses were shown to be elliptical in appearance in vivo

propagating from a single source (Nimmerjahn, et al. 2009). ATP diffuses from the site of release three dimensionally between astrocytes, a mechanism observed in both culture and intact brain across different brain regions (Arcuino, et al. 2002; Hoogland, et al. 2009). We had therefore hoped that pharmacological results in culture could be translated to intact slices from cerebellum. Instead, we found that the pharmacological profile was different, and so the outcome of culture experiments was not directly applicable to slice experiments.

When comparing data across the preparations, the broad spectrum blocking of P2 receptors with suramin and PPADS shows marked differences between the cortical astrocytes in culture and the Bergmann glia within slices (Figures 3.4 and 4.6). Pharmacological literature shows significant overlap of P2 receptor isoforms, spanning both P2Y and P2X receptors in the brain regions (Syed & Kennedy, 2011), but differences between astroglia types expressed across the brain regions is well documented and what makes the classification of astroglia difficult (Batiuk, et al. 2020). This heterogeneity of astrocytes phenotypes means difference subtypes of a receptor class is not uncommon across the range of glial cells.

5.2 Parallel fibre signalling to Bergmann glia

Bergmann glia respond to activity from the inputs of both parallel and climbing fibres to the Purkinje cells, through a combination of glutamate and ATP transmission (Beierlein & Regehr, 2006; Bellamy, 2006). The Bergmann glia therefore react to a combination of neurotransmitters and associates with multiple neuronal elements, this allows them in principle to regulate plasticity changes at each synapse and also over multiple synapses if the calcium signal spreads through large regions of the cerebellar cortex (Nimmerjahn, et al. 2009).

Glutamate signalling is recognised to be key in neuron to glia signalling in the cerebellum, with Bergmann glia expressing GluA2 deficient AMPA receptors for calcium permeability (Iino, et al. 2001; Bellamy & Ogden, 2005). In response to parallel fibre stimulation increases in membrane currents at the AMPA receptor are observed (Bellamy & Ogden, 2005; De Zeeuw & Hoogland. 2015). The calcium increases associated with AMPAR activation are rapid transients, mainly localised to the microdomains of the Bergmann glia (Hoogland & Kuhn, 2009; Araque, et al. 2014), and are thought to be associated with localised plasticity and proximity changes related to Bergmann glia's ability to envelop the synapse or parallel fibre. Furthermore, these local responses can help create a compartment for plasticity changes, in which calcium responses have a spatial threshold which focus glia modulation (Araque, et al. 2014).

Activation of glial AMPA receptors depends on ectopic transmission from parallel fibres, where vesicle fusion occurs outside the active zone, providing a dedicated pathway for neuron to astroglia signalling (Matsui et al. 2005). These ectopic sites are functionally independent to the synapse (Dobson & Bellamy, 2015), and previous work in the laboratory has shown that both short-term and long-term plasticity mechanisms exist for ectopic transmission (Bellamy, 2006; Croft, et al. 2015; Dobson, et al. 2018).

The origin for the ATP release during parallel fibre stimulation is still under discussion, with possibilities of interneuron and glial release (Beierlein & Regehr, 2006; Piet & Jahr, 2007; Nedergaard, et al. 2013). ATP release in the molecular layer depends on ionotropic glutamate receptor activation (Klyutch, et al. 2012) consistent with a neuronal or Bergmann glial source.

Although when stimulating Purkinje cells and interneurons, only the interneurons produced calcium transients in Bergmann glia, suggesting possible targeted ATP release (Piet & Jahr, 2007). Expression studies have previously shown the P2Y and P2X subtypes are present in Bergmann glia, offering metabotropic and ionotropic mechanisms for calcium signalling (Beierlein & Regehr, 2006, Habbas, et al. 2011).

We were able to reproduce the key observations about glutamate and ATP signalling in Bergmann glia in this project. Stimulating the parallel fibre at 30 Hz elicits a clear glial calcium response that spreads through the whole cell (see Figure 1.3). Whole cell recording is a technically demanding and time-consuming method, and so we developed a bulk-loading approach that allowed for identification of glial responses in the mixed signal obtained from the molecular layer. Here fluorescence climbs through the molecular layer perpendicular to parallel fibres, and a secondary peak is seen in the time course of fluorescence intensity that has closely similar kinetics to single cell responses (see Figure 4.3A, 4.4A).

Pharmacological study showed that these calcium responses in Bergmann glia could be reliably blocked by with a combination of AMPA antagonist, NBQX, selective mGlu1 antagonist, CPCCOEt and the P2 receptor antagonist PPADS (Figure 4.6), consistent with previous reports (Piet & Jahr, 2007; Beierlein & Regehr, 2006). In contrast to our investigation in primary cultures, suramin was ineffective at blocking Bergmann glial responses (Figure 4.6, 4.7).

Bulk loading of indicator clearly has limitations for isolation of the glial signal from surrounding neuronal elements. While the spatial pattern, kinetics and pharmacological sensitivity of the perpendicularly propagating signals correspond with whole cell recordings in single Bergmann glia, there is also a rapid neuronal calcium response observed in the method which is likely to be calcium influx into parallel fibres. A final test was to reproduce a preliminary observation from the laboratory that a tetanus used to induce long-term potentiation of parallel fibre synapses caused dramatic depression of Bergmann glial calcium signals (Figure 1.3). Using the LTP stimulus we were able to reproduce this phenomenon in bulk-loaded slices.

5.3 Depression of Bergmann glial calcium responses

16 Hz stimulation for 15s induces LTP at the parallel fibre synapse but displays a large depression of calcium responses observable in Bergmann glia after 30 Hz tetanus.

The mechanisms around the induction of LTP at the parallel fibre-Purkinje cell synapse occur at the presynaptic terminal. This potentiation at the parallel fibre not only increases the release probability but also the ability for multi-vesicular release (Bender, et al. 2009). Presynaptic LTP involves an increase in adenylate cyclase activity to increase the production of cAMP in turn activating Protein Kinase A (PKA) to phosphorylate release machinery (Salin, et al. 1996; Jacoby, et al. 2001). This is further reinforced by calcium dependent activation of Nitric Oxide Synthase (NOS) in the parallel fibres also potentiating neurotransmitter release (Jacoby, et al. 2001). Synaptic strength is modified in an activity dependent manner through these mechanisms, leading to long term increases in release probability. This can also lead to glutamate spill over to adjacent parallel fibre synapses (Salin, et al. 1996).

This stimulus protocol that induced LTP the Purkinje cell synapse produces the opposite effects in Bergmann glia. Previous investigation in single cell stimulation performed by the laboratory, observed that the calcium signal wave was not completely removed following 16Hz stimulation. Increased intracellular calcium concentration was present but stunted to the site of initiation, failing to show observable global signals or spread of calcium waves through the molecular layer (Figure 1.3). This spatial plasticity was reproducible in the slice imaging performed within this study, in which the calcium signal is not eliminated following 16Hz, although robustly knocked down, showing reduction in the signal propagation and glial recruitment (Figure 4.8).

The mechanism for this depression of Bergmann glial calcium signalling is unknown, but many neurotransmitter and neuromodulatory pathways are known to regulate neuron-glial transmission, including endocannabinoids, GABA, purines and nitric oxide (Dobson & Bellamy, 2015). Preliminary screening for these receptors with single cell recording failed to identify any antagonists at these receptors that blocked glial depression (unpublished results). One of the goals of this project was to speed up the identification of a possible plasticity mechanism using the bulk-loading method to screen candidates more efficiently. We applied this to test another neuromodulator candidate, serotonin.

Serotonergic signalling has been shown throughout the cerebellum and associates with LTD and LTP mechanisms of neuronal elements (Verge, et al. 1991). The neuronal system within the cerebellum receives serotonergic input originating from pontine raphe nucleus, pallidal raphe nucleus, dorsal raphe nucleus and median raphe nucleus in the midbrain (Kawashima, 2018).

The effects of serotonin signalling are mixed due to the range of receptor subtypes and the downstream mechanisms. In the cerebellum it has been shown that serotonin increased spontaneous spikes in the Purkinje neurons and decreased response to glutamate, and caused a long-term depression in parallel fibre to Purkinje cell synapses, modulating glutamatergic transmission in these instances (Kawashima, 2018). The modulation via serotonin in the instance of Purkinje neurons is theorised to be dependent on 5-HT_{1A} receptor subtypes exerting potent inhibition of the excitatory glutamate transmission - inhibiting AMPA glutamate downstream pathways (Strahlendorf & Hubbard, 1983; Takei, 2005). Activation of 5-HT_{1A} receptors reduces intracellular cyclic adenosine monophosphate (cAMP), opening K^+ channels for a hyperpolarization of the membrane which inhibits voltage gated Ca^{2+} channels necessary for exocytosis machinery (Wang, et al. 2012). It has also been shown that in neuropile glial cells that serotonin can hyperpolarise the cell in a calcium dependent manner, likely due to K^+ conductance in the glia (Laming, et al. 2000).

Staining investigations have shown concordance of 5-HT_{1A} receptor densities with maturation rates of Bergmann glia through the developing molecular layer (Verge, et al. 1991). This could be possibly involved in the development of neurons and maturation of the glial cell (Verge, et al. 1991; Miyazaki & Asanuma, 2016).

Increases in cerebellar serotonin originate from exocytotic release, observed in calcium depletion study, although some have extraneuronal origin to self-modulate through 5-HT_1 receptors (Mendelin, et al. 1996). Expression evidence for modulatory serotonergic transmission into the cerebellum on information processing is associated with Purkinje neuron sensitivity and firing rate (Mendelin, et al. 1996). This offers a pivotal role in modulating motor

learning and information processing of sensorimotor information for learned association of motor outputs (Fleming & Hull 2019). Serotonin elements have been shown to be integrated with super-learning hypothesis in the cerebellum as part of motor behaviour, associated with LTP and LTD, for fine tuning of granule cell and Purkinje neurons, and formation of microcomplexes modulated by serotoninergic projections (Caligiore, et al. 2019). The LTD and LTP relations of cerebellar neurons is complex and would predict a similar complexity in the Bergmann glia, and possibly interneurons.

Serotonin can also induce a calcium release in a very similar pathway to that of metabotropic glutamate and P2Y receptors. Cultured astrocytes expressing 5-HT_{2A} subtype demonstrate increases in intracellular calcium, through G_q protein coupling and increases of intracellular IP_3 for cytosolic calcium increases via ER (Fatima Shad & Saeed, 2007). Expression of serotonin receptors in Bergmann glia is uncertain, but mRNA expression has shown to include the calcium inducing 5-HT_{2A} receptor in cerebellum primary astrocytes (Hirst, et al. 1998). However, Bergmann glia fail to respond to serotonin in an intracellular calcium dependent manner under fluorescence investigation in slices (Kirishuck, et al. 1996). This does not completely rule out the instance of Bergmann glia expressing serotonergic receptors involved in the 16Hz parallel fibre LTD of subsequent 30Hz stimulations, or that serotonin can be acting on other cell classes.

Asenapine, a potent antipsychotic, has been recently highlighted as a potent 5-HT receptor antagonist, but also with a high affinity for α2 adrenergic and dopamine receptors (Frånberg, et al. 2008; Delcourte, et al. 2017). The broad-spectrum antagonising activity of asenapine allowed for the study of any serotonergic involvement in 16 Hz knockdown of proceeding 30 Hz stimuli.

Despite this evidence for a key role of serotonergic modulation of synaptic signalling in the cerebellum, within this study antagonising the serotonergic pathway with asenapine in slice preparation showed no significant reversal of the 16 Hz induced calcium response knockdown (Figure 4.9). There was an increase in mean response with asenapine treatment, but variation between experiments meant the significance of this cannot be reliably reported here and a conclusion would require a larger and more in-depth investigation into receptor subtype expression.

5.4 Future directions

The mechanism of Bergmann glial depression is still unknown, and several obvious neuromodulatory pathways have been ruled out. An alternative possibility is that the release of ATP is also depressed by 16 Hz stimulation and that loss of ATP is the cause of the impairment of glial calcium signalling. As the source of ATP is not known, there is also uncertainty about how ATP release is affected by LTP induction.

LTP in parallel fibre stimulation may alter the activation of interneurons. Interneuron ATP release could be inhibited affecting P2 activation on Bergmann glia, possibly inhibiting future glia response and propagation. 16 Hz stimulation could provide a knockdown mechanism from parallel fibres to either deplete or affect release probability at interneuronal and neuronal ectopic release sites. A good next step in the investigation would be to test this possibility.

The consequences of spatial plasticity are also unknown. The Bergmann Glia AMPA receptors dictate structural plasticity and formation of microdomains for glial modulation at the synapse (Iino, et al. 2001). This can lead to a modulation of signal transients at the synapse through increased proximity of glial uptake mechanisms or ion transporters inducing forms of short-term or long-term plasticity at the synapse. Such local signalling events should be intact despite the loss of widespread calcium propagation, suggesting that the impact of plasticity would be greater on glial functions that are more wide ranging.

Bergmann glia modulate ionic gradients at the synapse and have benefits in sustaining an increased neuronal activity through the redistribution of K^+ ions (De Zeeuw & Hoogland, 2015). Inward rectifying K^+ channels (KIR) effectively redistribute the ions into the Bergmann glia, playing an important role in modulating the K^+ concentrations for maintenance of Purkinje neuron membrane potentials (Butt & Kalsi, 2006). Increases in Bergmann glia calcium signalling are also linked to the ability to further regulate the extracellular K^+ uptake, aiding the neuronal output. Hyperpolarization through ionic gradients lead to an extended up-state of the neuron (Wang, et al. 2012). This mechanism is observed in vivo in awake state animals, differing from the oscillation states observed in sleep or anaesthesia (Wang, et al. 2012). The ability for Bergmann glia to affect the extracellular space occupied by the pre- and postsynaptic terminals allows for modulation of release probability and signalling transients (Wang, et al. 2012). Here induced glial LTD phenomenon could alter such widespread coordination of buffering, meaning the synaptic transients during activity at high frequencies at the synapse could be prolonged or increased through reduction of glial buffering and increased extracellular K^+ ions.

Our method for extracellular loading of the cerebellar slice allowed for a bulk loading of Bergmann glia without the difficulty or time-consuming manner of single cell loading. This protocol also allows for less disruption of the tissue in the site of imaging and for a greater number of loaded Bergmann glia in each slice compared to that of the single cell loading and stimulation. However, the extracellular loading methodology provides challenges in isolating glia response. The proximity and density of the molecular layer's cellular architecture, key for glia function, becomes a stumbling block for analysis. The overlapping parallel fibres that produce a rapid calcium response in relation to 30 Hz and a prolonged response in 16 Hz stimulation overlap with the Bergmann glia units that are perpendicular, creating interference when trying to isolate Bergmann glia calcium responses. This highlights that the use of bulk loading offers a unique perspective to that of astrocyte calcium signalling in slices, but complications in data and analysis outweigh the simplicities of the protocol. Therefore, investigations and data obtained through this methodology would have to be further supported with other investigation techniques such as single cell patch clamp.

The use of transgenic reporter mice expressing calcium sensitive fluorescent proteins is a superior method for monitoring calcium signalling in multiple glial cells (Paukert, et al. 2014). We did not have access to this technology within this investigation, but the use of these transgenic mice would eliminate the downsides to bulk loading. Recently the use of this, alongside photon microscopy, in live animals for visualization of in situ dynamics has provided a non-invasive method for monitoring calcium signalling in vivo. Genetically encoded calcium indicator (GECI) work has previously been used to investigate glial signalling (Atkin, et al. 2009; Stobart, et al. 2018). This approach would provide a more reliable report of the calcium signalling isolated to the Bergmann glia themselves.

Astrocyte calcium signalling has been investigated in that manner with considerable success in recent years. Stobart, et al. 2018 genetically added astrocytic (GCaMP6f) and neuronal (RCaMP1.07) genes for cellular structure identification and more discrete calcium signalling in microdomains highlighting astrocytes speed for involvement in synaptic plasticity. Furthermore, the use of transgenic lines co-labelling GFAP-GFP have previously been used to confirm Bergmann glia structure and could also aid in the identification of glia within acutely isolated cerebellar slices (Ango, et al. 2008; Lohr & Deitmer. 2010). Here glial-specific tags could provide an overlay image to define the boundaries of the Bergmann glia within raw images. Mapping of the glia of a slice for a machine learning process could aid analysis packages to recognise similar responses in data produced from the bulk loading protocol in slices.

Together, the extracellular bulk loading protocol used here provides a useful tool for efficiently screening pharmacological agents in relation to stimulation frequencies with its own strengths and weaknesses. It was possible to reproduce the spatial plasticity previously observed in Bergmann glia, to provide confidence in this protocol. The main suggestion would be to replace this with GECIs to strengthen the conclusion that the responses observed are glial only.

5.5 Concluding Remarks

Our work was able to provide several insights into the calcium signal propagation of astrocytes. Glutamate induced calcium responses in cultured cortical astrocytes are not reinforced to a significant extent by secondary signalling through purinoreceptors following ATP release. Pharmacological analysis suggested a possible negative feedback mechanism during prolonged stimulation with either glutamate or ATP, mediated by P2Y receptors. The pharmacological results from cultured cells could not be directly translated to intact cerebellar tissue slices, highlighting the need for in situ studies. A new bulk loading protocol was developed to investigate a spatial plasticity phenomenon of Bergmann glia, in which LTP at the parallel fibre induces an LTD response in glia. This protocol allowed for successful reproduction of this phenomenon but has strengths and weaknesses, and ultimately would benefit from use of genetic indicators in the future. Finally, the data obtained here showed no significant role for serotonin inputs to induce this glial plasticity and affect calcium signal propagation.

6 References

Alekseeva, O., Kirik, O., Gilerovich, E. and Korzhevskii, D., (2019). Microglia of the Brain: Origin, Structure, Functions. *Journal of Evolutionary Biochemistry and Physiology*, 55(4), pp.257-268.

Allen, N. and Lyons, D., (2018). Glia as architects of central nervous system formation and function. *Science*, 362(6411), pp.181-185.

Anderson, E., McFarland, D. and Kimelberg, H., (1992). Serotonin uptake by astrocytes in situ. *Glia*, 6(2), pp.154-158.

Ango, F., Wu, C., Van der Want, J., Wu, P., Schachner, M. and Huang, Z., (2008). Bergmann Glia and the Recognition Molecule CHL1 Organize GABAergic Axons and Direct Innervation of Purkinje Cell Dendrites. *PLoS Biology*, 6(4), p.e103.

Arcuino, G., Lin, J., Takano, T., Liu, C., Jiang, L., Gao, Q., Kang, J. and Nedergaard, M., (2002). Intercellular calcium signaling mediated by point-source burst release of ATP. *Proceedings of the National Academy of Sciences*, 99(15), pp.9840-9845.

Araque, A., Parpura, V., Sanzgiri, R. and Haydon, P., (1999). Tripartite synapses: glia, the unacknowledged partner. *Trends in Neurosciences*, 22(5), pp.208-215.

Araque, A., Carmignoto, G., Haydon, P., Oliet, S., Robitaille, R. and Volterra, A. (2014). Gliotransmitters Travel in Time and Space. *Neuron*, 81(4), pp.728-739.

Araujo, A., Carpi-Santos, R. and Gomes, F. (2019). The Role of Astrocytes in the Development of the Cerebellum. *The Cerebellum*.

Atkin, S., Patel, S., Kocharyan, A., Holtzclaw, L., Weerth, S., Schram, V., Pickel, J. and Russell, J., (2009). Transgenic mice expressing a cameleon fluorescent Ca2+ indicator in astrocytes and Schwann cells allow study of glial cell Ca2+ signals in situ and in vivo. *Journal of Neuroscience Methods*, 181(2), pp.212-226.

Batiuk, M., Martirosyan, A., Wahis, J., de Vin, F., Marneffe, C., Kusserow, C., Koeppen, J., Viana, J., Oliveira, J., Voet, T., Ponting, C., Belgard, T. and Holt, M., (2020). Identification of region-specific astrocyte subtypes at single cell resolution. *Nature Communications*, 11(1).

Baxter, P. and Hardingham, G., (2016). Adaptive regulation of the brain's antioxidant defences by neurons and astrocytes. *Free Radical Biology and Medicine*, 100, pp.147-152.

Bayraktar, O., Fuentealba, L., Alvarez-Buylla, A. and Rowitch, D., (2014). Astrocyte Development and Heterogeneity. *Cold Spring Harbor Perspectives in Biology*, 7(1), p.a020362.

Beamer, E., Kovács, G. and Sperlágh, B. (2017). ATP released from astrocytes modulates action potential threshold and spontaneous excitatory postsynaptic currents in the neonatal rat prefrontal cortex. *Brain Research Bulletin*, 135, pp.129-142.

Beierlein, M. and Regehr, W. (2006). Brief Bursts of Parallel Fiber Activity Trigger Calcium Signals in Bergmann Glia. *Journal of Neuroscience*, 26(26), pp.6958-6967.

Beierlein, M., (2013). Imaging Calcium Waves in Cerebellar Bergmann Glia. *Cold Spring Harbor Protocols*, 2013(1), pp.pdb.prot072637-pdb.prot072637.

Bélanger, M., Allaman, I. and Magistretti, P., (2011). Brain Energy Metabolism: Focus on Astrocyte-Neuron Metabolic Cooperation. *Cell Metabolism*, 14(6), pp.724-738.

Bellamy, T. and Ogden, D. (2005). Short-term plasticity of Bergmann glial cell extrasynaptic currents during parallel fiber stimulation in rat cerebellum. *Glia*, 52(4), pp.325-335.

Bellamy, T. (2006). Interactions between Purkinje neurones and Bergmann glia. *The Cerebellum*, 5(2), pp.116-126.

Bender, V., Pugh, J. and Jahr, C., (2009). Presynaptically Expressed Long-Term Potentiation Increases Multivesicular Release at Parallel Fiber Synapses. *Journal of Neuroscience*, 29(35), pp.10974-10978.

Bohmbach, K., Schwarz, M., Schoch, S. and Henneberger, C. (2018). The structural and functional evidence for vesicular release from astrocytes in situ. *Brain Research Bulletin*, 136, pp.65-75.

Boison, D., Chen, J. and Fredholm, B., (2009). Adenosine signaling and function in glial cells. *Cell Death & Differentiation*, 17(7), pp.1071-1082.

Brenowitz, S. and Regehr, W., (2014). Presynaptic Calcium Measurements Using Bulk Loading of Acetoxymethyl Indicators. *Cold Spring Harbor Protocols*, 2014(7), pp.pdb.prot081828-pdb.prot081828.

Brockhaus, J. and Deitmer, J., (2002). Long-lasting modulation of synaptic input to Purkinje neurons by Bergmann glia stimulation in rat brain slices. *The Journal of Physiology*, 545(2), pp.581-593.

Brown, A. and Ransom, B., (2007). Astrocyte glycogen and brain energy metabolism. *Glia*, 55(12), pp.1263-1271.

Buffo, A. and Rossi, F. (2013). Origin, lineage and function of cerebellar glia. *Progress in Neurobiology*, 109, pp.42-63.

Butt, A. and Kalsi, A. (2006). Inwardly rectifying potassium channels (Kir) in central nervous system glia: a special role for Kir4.1 in glial functions. *Journal of Cellular and Molecular Medicine*, 10(1), pp.33-44.

Caesar, K., Hashemi, P., Douhou, A., Bonvento, G., Boutelle, M., Walls, A. and Lauritzen, M., (2008). Glutamate receptor-dependent increments in lactate, glucose and oxygen metabolism evoked in rat cerebellumin vivo. *The Journal of Physiology*, 586(5), pp.1337-1349.

Caligiore, D., Arbib, M., Miall, R. and Baldassarre, G. (2019). The super-learning hypothesis: Integrating learning processes across cortex, cerebellum and basal ganglia. *Neuroscience & Biobehavioral Reviews*, 100, pp.19-34.

Chever, O., Lee, C. and Rouach, N. (2014). Astroglial Connexin43 Hemichannels Tune Basal Excitatory Synaptic Transmission. *Journal of Neuroscience*, 34(34), pp.11228-11232.

Cornell-Bell, A., Finkbeiner, S., Cooper, M. and Smith, S. (1990). Glutamate induces calcium waves in cultured astrocytes: long-range glial signaling. *Science*, 247(4941), pp.470-473.

Croft, W., Dobson, K. and Bellamy, T. (2015). Plasticity of Neuron-Glial Transmission: Equipping Glia for Long-Term Integration of Network Activity. *Neural Plasticity*, 2015, pp.1-11.

Croft, W., Reusch, K., Tilunaite, A., Russell, N., Thul, R. and Bellamy, T. (2016). Probabilistic encoding of stimulus strength in astrocyte global calcium signals. *Glia*, 64(4), pp.537-552.

David, J., Yamada, K., Bagwe, M. and Goldberg, M. (1996). AMPA receptor activation is rapidly toxic to cortical astrocytes when desensitization is blocked. *The Journal of Neuroscience*, 16(1), pp.200-209.

Delcourte, S., Abrial, E., Etiévant, A., Rovera, R., Arnt, J., Didriksen, M. and Haddjeri, N. (2017). Asenapine modulates mood-related behaviors and 5-HT1A/7 receptors-mediated neurotransmission. *CNS Neuroscience & Therapeutics*, 23(6), pp.518-525.

De Zeeuw, C. and Hoogland, T. (2015). Reappraisal of Bergmann glial cells as modulators of cerebellar circuit function. *Frontiers in Cellular Neuroscience*, 9.

Dieudonné, S., (2001). Book Review: Serotonergic Neuromodulation in the Cerebellar Cortex: Cellular, Synaptic, and Molecular Basis. *The Neuroscientist*, 7(3), pp.207-219.

Ding, S., Fellin, T., Zhu, Y., Lee, S., Auberson, Y., Meaney, D., Coulter, D., Carmignoto, G. and Haydon, P. (2007). Enhanced Astrocytic Ca2+ Signals Contribute to Neuronal Excitotoxicity after Status Epilepticus. *Journal of Neuroscience*, 27(40), pp.10674-10684.

Dobson, K. and Bellamy, T. (2015). Localization of Presynaptic Plasticity Mechanisms Enables Functional Independence of Synaptic and Ectopic Transmission in the Cerebellum. *Neural Plasticity*, 2015, pp.1-11.

Dobson, K., Smith, Z. and Bellamy, T. (2018). Distribution of vesicle pools in cerebellar parallel fibre terminals after depression of ectopic transmission. *PLOS ONE*, 13(7), p.e0200937.

Fages, C., Le Prince, G., Didier-Bazes, M., Rolland, B., Hardin, H. and Tardy, M., (1994). Long-term astroglial reaction to serotonergic fiber degeneration. *Brain Research*, 639(1), pp.161-166.

Fatima Shad, K. and Saeed, S. (2007). The metabolism of serotonin in neuronal cells in culture and platelets. *Experimental Brain Research*, 183(3), pp.411-416.

Fleischer, W., Theiss, S., Slotta, J., Holland, C. and Schnitzler, A. (2015). High-frequency voltage oscillations in cultured astrocytes. *Physiological Reports*, 3(5), p.e12400.

Fleming, E. and Hull, C. (2019). Serotonin regulates dynamics of cerebellar granule cell activity by modulating tonic inhibition. *Journal of Neurophysiology*, 121(1), pp.105-114.

Foerster, S., Hill, M. and Franklin, R., (2019). Diversity in the oligodendrocyte lineage: Plasticity or heterogeneity?. *Glia*, 67(10), pp.1797-1805.

Frånberg, O., Wiker, C., Marcus, M., Konradsson, Å., Jardemark, K., Schilström, B., Shahid, M., Wong, E. and Svensson, T. (2007). Asenapine, a novel psychopharmacologic agent: preclinical evidence for clinical effects in schizophrenia. *Psychopharmacology*, 196(3), pp.417-429.

Franke, H., Krügel, U. and Illes, P., 1999. P2 receptor-mediated proliferative effects on astrocytes in vivo. *Glia*, 28(3), pp.190-200.

Fumagalli, M., Brambilla, R., D'Ambrosi, N., Volonté, C., Matteoli, M., Verderio, C. and Abbracchio, M. (2003). Nucleotide-mediated calcium signaling in rat cortical astrocytes: Role of P2X and P2Y receptors. *Glia*, 43(3), pp.218-230.

Grosche, J., Kettenmann, H. and Reichenbach, A. (2002). Bergmann glial cells form distinct morphological structures to interact with cerebellar neurons. *Journal of Neuroscience Research*, 68(2), pp.138-149.

Guthrie, P., Knappenberger, J., Segal, M., Bennett, M., Charles, A. and Kater, S. (1999). ATP Released from Astrocytes Mediates Glial Calcium Waves. *The Journal of Neuroscience*, 19(2), pp.520-528.

Habbas, S., Ango, F., Daniel, H. and Galante, M., (2011). Purinergic signaling in the cerebellum: Bergmann glial cells express functional ionotropic P2X7 receptors. *Glia*, 59(12), pp.1800-1812.

Harada, K., Kamiya, T. and Tsuboi, T., (2016). Gliotransmitter Release from Astrocytes: Functional, Developmental, and Pathological Implications in the Brain. *Frontiers in Neuroscience*, 9.

Hartell, N. (2002). Parallel fiber plasticity. *The Cerebellum*, 1(1), pp.3-18.

Hibi, M. and Shimizu, T., (2012). Development of the cerebellum and cerebellar neural circuits. *Developmental Neurobiology*, 72(3), pp.282-301.

Hirst, W., Cheung, N., Rattray, M., Price, G. and Wilkin, G. (1998). Cultured astrocytes express messenger RNA for multiple serotonin receptor subtypes, without functional coupling of 5-HT1 receptor subtypes to adenylyl cyclase. *Molecular Brain Research*, 61(1-2), pp.90-99.

Hoogland, T., Civillico, E. and Kuhn, B. (2007). Molecular Layer Interneurons Relay Cerebellar Cortical Activity to Bergmann Glial Cells. *Journal of Neuroscience*, 27(42), pp.11167-11169.

Hoogland, T. and Kuhn, B. (2009). Recent Developments in the Understanding of Astrocyte Function in the Cerebellum In Vivo. *The Cerebellum*, 9(3), pp.264-271.

Hoogland, T., Kuhn, B., Gobel, W., Huang, W., Nakai, J., Helmchen, F., Flint, J. and Wang, S. (2009). Radially expanding transglial calcium waves in the intact cerebellum. *Proceedings of the National Academy of Sciences*, 106(9), pp.3496-3501.

Iino, M., Goto, K., Kakegawa, W., Okado, H., Sudo, M., Ishiuchi, S., Miwa, A., Takayasu, Y., Saito, I., Tsuzuki, K. and Ozawa, S. (2001). Glia-Synapse Interaction Through Ca2+-Permeable AMPA Receptors in Bergmann Glia. *Science*, 292(5518), pp.926-929.

Ikeda, H., Kiritoshi, T. and Murase, K. (2012). Contribution of Microglia and Astrocytes to the Central Sensitization, Inflammatory and Neuropathic Pain in the Juvenile Rat. *Molecular Pain*, 8, pp.1744-8069-8-43.

Jacob, P., Vaz, S., Ribeiro, J. and Sebastião, A. (2014). P2Y1 receptor inhibits GABA transport through a calcium signalling-dependent mechanism in rat cortical astrocytes. *Glia*, 62(8), pp.1211-1226.

Jacoby, S., Sims, R. and Hartell, N., (2001). Nitric oxide is required for the induction and heterosynaptic spread of long-term potentiation in rat cerebellar slices. *The Journal of Physiology*, 535(3), pp.825-839.

Jäkel, S. and Dimou, L., (2017). Glial Cells and Their Function in the Adult Brain: A Journey through the History of Their Ablation. *Frontiers in Cellular Neuroscience*, 11(24).

James, G. and Butt, A. (2002). P2Y and P2X purinoceptor mediated Ca2+ signalling in glial cell pathology in the central nervous system. *European Journal of Pharmacology*, 447(2-3), pp.247-260.

James, L., Andrews, S., Walker, S., de Sousa, P., Ray, A., Russell, N. and Bellamy, T., (2011). High-Throughput Analysis of Calcium Signalling Kinetics in Astrocytes Stimulated with Different Neurotransmitters. *PLoS ONE*, 6(10), p.e26889.

Kawashima, T. (2018). The role of the serotonergic system in motor control. *Neuroscience Research*, 129, pp.32-39.

Kirischuk, S., Tuschick, S., Verkhratsky, A. and Kettenmann, H. (1996). Calcium Signalling in Mouse Bergmann Glial Cells Mediated by α1-adrenoreceptors and H1Histamine -Receptors. *European Journal of Neuroscience*, 8(6), pp.1198-1208.

Klyuch, B., Dale, N. and Wall, M., (2012). Deletion of Ecto-5'-Nucleotidase (CD73) Reveals Direct Action Potential-Dependent Adenosine Release. *Journal of Neuroscience*, 32(11), pp.3842-3847.

Kofuji, P. and Araque, A., (2021). G-Protein-Coupled Receptors in Astrocyte–Neuron Communication. *Neuroscience*, 456, pp.71-84.

Lalo, U., Pankratov, Y., Kirchhoff, F., North, R. and Verkhratsky, A. (2006). NMDA Receptors Mediate Neuron-to-Glia Signaling in Mouse Cortical Astrocytes. *Journal of Neuroscience*, 26(10), pp.2673-2683.

Lalo, U., Pankratov, Y., Wichert, S., Rossner, M., North, R., Kirchhoff, F. and Verkhratsky, A. (2008). P2X1 and P2X5 Subunits Form the Functional P2X Receptor in Mouse Cortical Astrocytes. *Journal of Neuroscience*, 28(21), pp.5473-5480.

Laming, P., Kimelberg, H., Robinson, S., Salm, A., Hawrylak, N., Müller, C., Roots, B. and Ng, K. (2000). Neuronal–glial interactions and behaviour. *Neuroscience & Biobehavioral Reviews*, 24(3), pp.295-340.

Lanner, J., Georgiou, D., Joshi, A. and Hamilton, S., (2010). Ryanodine Receptors: Structure, Expression, Molecular Details, and Function in Calcium Release. *Cold Spring Harbor Perspectives in Biology*, 2(11), pp.a003996-a003996.

Lippman Bell, J., Lordkipanidze, T., Cobb, N. and Dunaevsky, A. (2010). Bergmann glial ensheathment of dendritic spines regulates synapse number without affecting spine motility. *Neuron Glia Biology*, 6(3), pp.193-200.

Lohr, C. and Deitmer, J., (2009). Ca2+ Imaging of Glia. *Neuromethods*, pp.221-249.

MacMillan, D., Kennedy, C. and McCarron, J., (2012). ATP inhibits Ins(1,4,5)P3-evoked Ca2+ release in smooth muscle via P2Y1 receptors. *Journal of Cell Science*, 125(21), pp.5151-5158.

Matsui, K., Jahr, C. and Rubio, M., (2005). High-Concentration Rapid Transients of Glutamate Mediate Neural-Glial Communication via Ectopic Release. *Journal of Neuroscience*, 25(33), pp.7538-7547.

Matsui, K. and Jahr, C. (2006). Exocytosis unbound. *Current Opinion in Neurobiology*, 16(3), pp.305-311.

Miyazaki, I. and Asanuma, M. (2016). Serotonin 1A Receptors on Astrocytes as a Potential Target for the Treatment of Parkinson's Disease. *Current Medicinal Chemistry*, 23(7), pp.686-700.

Murphy-Royal, C., Dupuis, J., Varela, J., Panatier, A., Pinson, B., Baufreton, J., Groc, L. and Oliet, S., (2015). Surface diffusion of astrocytic glutamate transporters shapes synaptic transmission. *Nature Neuroscience*, 18(2), pp.219-226.

Nedergaard, M., Ransom, B. and Goldman, S. (2003). New roles for astrocytes: Redefining the functional architecture of the brain. *Trends in Neurosciences*, 26(10), pp.523-530.

Nimmerjahn, A., Mukamel, E. and Schnitzer, M. (2009). Motor Behavior Activates Bergmann Glial Networks. *Neuron*, 62(3), pp.400-412

Pangršič, T., Potokar, M., Stenovec, M., Kreft, M., Fabbretti, E., Nistri, A., Pryazhnikov, E., Khiroug, L., Giniatullin, R. and Zorec, R., (2007). Exocytotic Release of ATP from Cultured Astrocytes. *Journal of Biological Chemistry*, 282(39), pp.28749-28758.

Parpura, V. and Zorec, R. (2010). Gliotransmission: Exocytotic release from astrocytes. *Brain Research Reviews*, 63(1-2), pp.83-92.

Parpura, V., Grubišić, V. and Verkhratsky, A., (2011). Ca2+ sources for the exocytotic release of glutamate from astrocytes. *Biochimica et Biophysica Acta (BBA) - Molecular Cell Research*, 1813(5), pp.984-991.

Paukert, M., Agarwal, A., Cha, J., Doze, V., Kang, J. and Bergles, D., (2014). Norepinephrine Controls Astroglial Responsiveness to Local Circuit Activity. *Neuron*, 82(6), pp.1263-1270.

Peng, L., Huang, R., Yu, A., Fung, K., Rathbone, M. and Hertz, L., (2005). Nucleoside transporter expression and function in cultured mouse astrocytes. *Glia*, 52(1), pp.25-35.

Perea, G. and Araque, A., (2005). Properties of Synaptically Evoked Astrocyte Calcium Signal Reveal Synaptic Information Processing by Astrocytes. *Journal of Neuroscience*, 25(9), pp.2192-2203.

Perea, G., Navarrete, M. and Araque, A. (2009). Tripartite synapses: astrocytes process and control synaptic information. *Trends in Neurosciences*, 32(8), pp.421-431.

Pestana, F., Edwards-Faret, G., Belgard, T., Martirosyan, A. and Holt, M., (2020). No Longer Underappreciated: The Emerging Concept of Astrocyte Heterogeneity in Neuroscience. *Brain Sciences*, 10(3), p.168.

Piet, R. and Jahr, C. (2007). Glutamatergic and Purinergic Receptor-Mediated Calcium Transients in Bergmann Glial Cells. *Journal of Neuroscience*, 27(15), pp.4027-4035.

Riquelme, R., Miralles, C. and De Blas, A. (2002). Bergmann Glia GABAA Receptors Concentrate on the Glial Processes That Wrap Inhibitory Synapses. *The Journal of Neuroscience*, 22(24), pp.10720-10730.

Rose, C. and Kirchhoff, F., (2015). Glial heterogeneity: the increasing complexity of the brain. *e-Neuroforum*, 21(3), pp.59-62.

Rose, C., Felix, L., Zeug, A., Dietrich, D., Reiner, A. and Henneberger, C., (2018). Astroglial Glutamate Signaling and Uptake in the Hippocampus. *Frontiers in Molecular Neuroscience*, 10(451).

Salin, P., Malenka, R. and Nicoll, R., (1996). Cyclic AMP Mediates a Presynaptic Form of LTP at Cerebellar Parallel Fiber Synapses. *Neuron*, 16(4), pp.797-803.

Schipke, C., Haas, B. and Kettenmann, H., (2008). Astrocytes Discriminate and Selectively Respond to the Activity of a Subpopulation of Neurons within the Barrel Cortex. *Cerebral Cortex*, 18(10), pp.2450-2459.

Stobart, J., Ferrari, K., Barrett, M., Glück, C., Stobart, M., Zuend, M. and Weber, B. (2018). Cortical Circuit Activity Evokes Rapid Astrocyte Calcium Signals on a Similar Timescale to Neurons. *Neuron*, 98(4), pp.726-735.e4.

Strahlendorf, J. and Hubbard, G. (1983). Serotonergic interactions with rat cerebellar Purkinje cells. *Brain Research Bulletin*, 11(2), pp.265-269.

Svobodova, I., Bhattaracharya, A., Ivetic, M., Bendova, Z. and Zemkova, H. (2018). Circadian ATP Release in Organotypic Cultures of the Rat Suprachiasmatic Nucleus Is Dependent on P2X7 and P2Y Receptors. *Frontiers in Pharmacology*, 9.

Syed, N. and Kennedy, C. (2011). Pharmacology of P2X receptors. *Wiley Interdisciplinary Reviews: Membrane Transport and Signaling*, 1(1), pp.16-30.

Takano, T., Tian, G., Peng, W., Lou, N., Libionka, W., Han, X. and Nedergaard, M., (2005). Astrocyte-mediated control of cerebral blood flow. *Nature Neuroscience*, 9(2), pp.260-267.

Takeda, H., Inazu, M. and Matsumiya, T., (2002). Astroglial dopamine transport is mediated by norepinephrine transporter. *Naunyn-Schmiedeberg's Archives of Pharmacology*, 366(6), pp.620-623.

Verderio, C., Cagnoli, C., Bergami, M., Francolini, M., Schenk, U., Colombo, A., Riganti, L., Frassoni, C., Zuccaro, E., Danglot, L., Wilhelm, C., Galli, T., Canossa, M. and Matteoli, M., (2012). TI-VAMP/VAMP7 is the SNARE of secretory lysosomes contributing to ATP secretion from astrocytes. *Biology of the Cell*, 104(4), pp.213-228.

Verkhratsky, A. and Nedergaard, M., (2018). Physiology of Astroglia. *Physiological Reviews*, 98(1), pp.239-389.

Verge, D., Matthiessen, L., Daval, G., Bailly, Y., Kia, H. and Hamon, M. (1991). Localization of 5-HT1A serotonin receptors in the cerebellum of young rats. *Neurochemistry International*, 19(4), pp.425-431.

Wang, F., Smith, N., Xu, Q., Fujita, T., Baba, A., Matsuda, T., Takano, T., Bekar, L. and Nedergaard, M. (2012). Astrocytes Modulate Neural Network Activity by Ca2+-Dependent Uptake of Extracellular K+. *Science Signaling*, 5(218), pp.ra26-ra26.